

Significant Role of DNA Backbone in Mediating the Transition Origin of Electronic Excitations of B-DNA – Implication from Long Range Corrected TDDFT and Quantified NTO Analysis

Jian-Hao Li^{a, b}, Jeng-Da Chai^{a, c, *}, Guang-Yu Guo^{a, c, d}, Michitoshi Hayashi^{b, *}

^aDepartment of Physics, Center for Theoretical Sciences, National Taiwan University, Taipei 10617, Taiwan.

^bCenter for Condensed Matter Sciences, National Taiwan University, Taipei 10617, Taiwan.

^cCenter for Quantum Science and Engineering, National Taiwan University, Taipei 10617, Taiwan.

^dGraduate Institute of Applied Physics, National Chengchi University, Taipei 11605, Taiwan

E-mail: jdchai@phys.ntu.edu.tw (J.-D. Chai); atmyh@ntu.edu.tw (M. Hayashi)

2nd November 2011

We systematically investigate the possible complex transition origin of electronic excitations of giant molecular systems by using the recently proposed QNTO analysis [J.-H. Li, J.-D. Chai, G. Y. Guo and M. Hayashi, *Chem. Phys. Lett.*, 2011, **514**, 362.] combined with long-range corrected TDDFT calculations. Thymine (Thy) related excitations of biomolecule B-DNA are then studied as examples, where the model systems have been constructed extracting from the perfect or a X-ray crystal (PDB code 3BSE) B-DNA structure with at least one Thy included. In the first part, we consider the systems composed of a core molecular segment (e.g. Thy, di-Thy) and a surrounding physical/chemical environment of interest (e.g. backbone, adjacent stacking nucleobases) and examine how the excitation properties of the core vary in response to the environment. We find that the orbitals contributed from DNA backbone and surrounding nucleobases often participate in a transition of Thy-related excitations affecting their composition, absorption energy, and oscillator strength. In the second part, we take into account geometrically induced variation of the excitation properties of various B-DNA segments, e.g. di-Thy, dTpdT etc., obtained from different sources (ideal and 3BSE). It is found that the transition origin of several Thy-related excitations of these segments is sensitive to slight conformational variations, suggesting that DNA with thermal motions in cells may from time to time exhibit very different photo-induced physical and/or chemical processes.

1. Introduction

The primary functions of DNA molecules to encode cellular genetic information and to engage in replication have readily rendered them to be the most important biomolecules^{1, 2}. Investigation on them has long been a hot topic to date such that a great deal of understanding has been advanced on their mechanisms, physical properties, chemical properties etc. and possible application in nanotechnology³⁻⁶. Among all the important issues on DNA, one is related to their optical absorption spectroscopy. It has been well-known that the optical absorption spectra of nucleobases – thymine, adenine, cytosine, guanine – or different combinations of them are dominated by bright $^1\pi\pi^*$ excitations interlaced with dark $^1n\pi^*$ ones in the ultraviolet range⁷⁻³⁵. Its related experimental and theoretical studies can be reviewed, for example, in an excellent collection³⁶; several quantum chemistry methods, like configuration interaction singles (CIS)³⁷⁻⁴³, complete active space self-consistent-field with multiconfigurational second order perturbation theory (CASPT2/CASSCF)⁴⁴⁻⁴⁶, second-order approximate coupled-cluster theory with the resolution-of-the-identity approximation (RI-CC2)⁴⁷⁻⁴⁸, time-dependent DFT (TDDFT)⁴⁹⁻⁵⁷ or etc. have been used in literature.

In order to know more about how nucleobases alter their excitation properties in response to surrounding environment within a giant complex DNA molecule, however, it is still a formidable task nowadays employing high-level quantum chemistry approaches, like equation of motion coupled cluster singles and doubles (EOM-CCSD)⁵⁸⁻⁶⁰ and etc., to directly simulate a huge system composed of the core part and the interesting environment. TDDFT⁶¹⁻⁶⁴, on the other hand, may currently be the only choice that can deal with large size

molecular systems at the same time with less computational difficulty, although the correctness of output can be a debate.

In practice, model potentials and/or embedded system schemes are often employed to divide the whole system into many sub-layers/sub-systems handled by separate theoretical treatments⁶⁵⁻⁸⁰. In this way, interesting local excitations of a core subsystem embedded in an environment can be sophisticatedly described. However, a noticeable drawback is that orbital transitions from/to environments are not allowed. Fortunately, a direct simulation of giant molecular systems by (TD-)DFT has recently become feasible and reliable due to the great progress on the development of long-range corrected (LC) hybrid functionals⁸¹⁻⁹⁴. In this case, effects of such orbital transitions can be feasibly included.

In the LC hybrid scheme, the Coulomb operator is first split into a long-range (LR) operator $L(r_{12})/r_{12}$ and a complementary short-range (SR) operator $[1-L(r_{12})]/r_{12}$,

$$\frac{1}{r_{12}} = \frac{L(r_{12})}{r_{12}} + \frac{[1-L(r_{12})]}{r_{12}} \quad (1)$$

where $L(r_{12})$ is a function of inter-electronic separation $r_{12} \equiv |\mathbf{r}_{12}| = |\mathbf{r}_1 - \mathbf{r}_2|$, ranging from 0 to 1, and approaching to 1 at large r_{12} . Currently, the most popular $L(r_{12})$ used in the LC hybrid scheme is the standard error function (erf), although there are several variants as well.

After the splitting, the LR part of exchange is treated exactly by Hartree-Fock (HF) theory (where $\gamma_\sigma(\mathbf{r}_1, \mathbf{r}_2)$ is the one-electron spin density matrix),

$$E_x^{LR-HF} = -\frac{1}{2} \sum_\sigma \iint L(r_{12}) \frac{|\gamma_\sigma(\mathbf{r}_1, \mathbf{r}_2)|^2}{r_{12}} d\mathbf{r}_1 d\mathbf{r}_2 \quad (2)$$

the SR part of exchange is treated by density functional approxi-

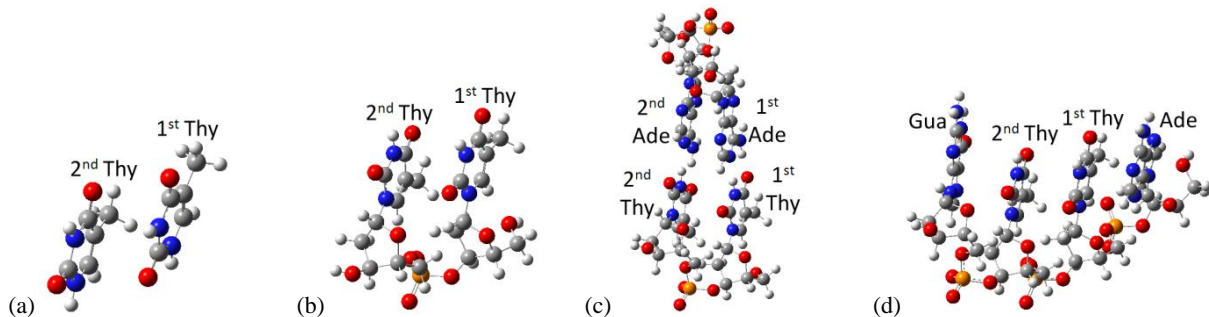


Fig. 1 Various Thy-comprised systems extracted from ideal B-DNA: (a) two thymines (di-Thy), (b) two thymines connected by DNA backbone (dTpdT), (c) dTpdT with WC pairing nucleobases (dTpdT--dApdA), and (f) dTpdT with adjacent stacking nucleobases (dApdTpdTpG). The order of bases is counted from 5'-end to 3'-end of the DNA strand.

mations (DFAs) (e.g. LDA or GGAs), and the correlation (also treated by DFAs) remains the same as that of the full Coulomb interaction,

$$E_{xc}^{LC-DFA} = E_x^{LR-HF} + E_x^{SR-DFA} + E_c^{DFA} \quad (3)$$

In recent years, LC hybrid functionals have gained increasing attentions due to their success in several important applications⁸³⁻⁸⁶.

In addition, we have lately proposed quantified natural transition orbital (QNTO) analysis⁹⁵ which is able to clearly exhibit the transition origin of electronic excitations. This framework should be especially useful for treating large biomolecules with high orbital energy density, where even the low-lying excitations are generally composed of several singly excited configurations (SECs) with similar weights pairing different occupied and unoccupied orbitals in the linear combination of SECs (LCSEC). This situation may be more commonplace particularly for DNA systems that consist of many similar molecular segments. Under such circumstances, QNTO analysis can often lead to one or two dominant SECs corresponding to NTO1 and NTO2 in the NTO-based LCSEC. Here NTO1(2) stands for the first (second) dominant NTO pair. The NTO1(2) can then be interpreted in terms of a standard-orbitals set chosen depending on the type of systems or chemical interest; for example, if any important photo-induced chemical reaction takes place in a dimer system, orbitals from monomer segment can be chosen as standard-orbitals. In other words, the transition origin of an electronic excitation of dimer can be interpreted by the monomer orbitals.

Thus, in light of the above two developments, the present work is in an effort by using TDDFT with LC hybrid functionals (LC-TDDFT) and QNTO analysis to systematically investigate the electronic excitations of giant molecular systems, here the DNA, in which orbitals exchange between core-subsystem and environment can be important.

We choose a Thy-appearing region of B-DNA (the commonest cellular form of DNA)⁹⁶ as an example and focus on its Thy-related excitations in which hole- and electron-orbitals are both significantly contributed from Thy. We study how different surrounding environments can play a role to its transition origin, absorption energy and oscillator strength. This is accomplished by extracting various B-DNA segments (nucleobases or oligonucleotides) with different environmental factors existing in vicinity of a Thy and by looking into their respective electronic

excitation properties. Moreover, the excitation properties of B-DNA segments obtained from different sources (ideal and 3BSE) are compared with each other to investigate conformational effect as well.

Recently, Kozak *et al.* have reported a thorough study⁹⁷ on the singlet electronic excitations of two π -stacked Thys through implementing a variety of quantum chemistry methods, including CIS, CIS(2), EOM-CCSD, TDDFT and CASSCF, based on molecular exciton theory⁹⁸. It is found that the coupling of Thy monomer orbitals to form dimer orbitals strongly depend on the distance and the relative orientation of two Thys. However, we have shown by using QNTO analysis⁹⁵ that for a real dimer system with low or no symmetry, such as two π -stacked Thys extracted from B-DNA, two local orbital transitions can no longer equally contribute to an electronic excitation predicted by the molecular exciton theory. If the dimer separation is short enough, the additional charge transfer (CT) contribution can also exist. Under such circumstances, QNTO can be a powerful tool to study the transition origins of electronic excitations that may consist of local or CT transition components in such a low-symmetry situation which is commonplace in median and large bio-molecular systems. Lange and Herbert⁹⁹ have also applied TDDFT with LC hybrid functionals to obtain the accurate absorption energies of interbase CT electronic excitations that are underestimated by TDDFT calculation with pure (e.g. LDA) or global hybrid (e.g. B3LYP) density functionals. Since both of the two reports focus on bare nucleobases model systems, a remaining question of interest is indeed whether the environmental factors like backbone to what extent affect the electronic excitations of nucleobases.

The paper is organized as follows. In section 2, computational procedures are introduced, where the preparation of various B-DNA sliced systems and DFT/TDDFT calculation details are presented. In subsection 3.1, the interpretation of the excitation properties of various systems calculated by TDDFT with QNTO analysis are introduced. Subsections 3.2~3.6 compare the results of various systems such that the influence of different environmental factors, i.e. the presence of another Thy, backbone, Watson Crick (WC) pairing nucleobases and stacking nucleobases, and conformational variation to the Thy-related excitations is successively focused on. Subsection 3.7 demonstrates the overall backbone influence to several low-lying excitations (not particularly Thy-related ones) of the systems consisting of backbone structure. Conclusion is given in Sec. 4.

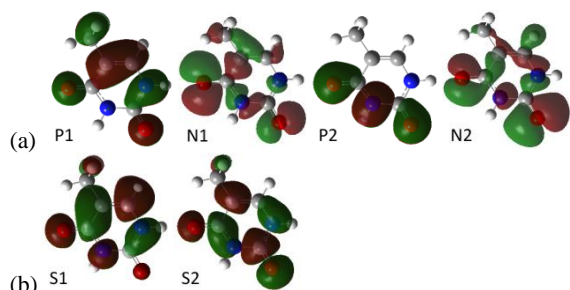


Fig. 2 Standard-orbitals of Thy generated in the B3LYP-DFT calculation. Isovalue=0.02 is adopted for the graphical representation. P1, N1, P2 and N2 correspond to the HOMO, HOMO-1, HOMO-2, and HOMO-3, respectively, and S1 and S2 are the LUMO and LUMO+1. The P1 and P2 are from the components of ${}^1\pi\pi^*$ -character excitations while N1 and N2 those from ${}^1n\pi^*$ -character excitations.

2. Computational Details

2.1. Preparation and TDDFT Calculations of Thy-comprised Molecules

Various molecular systems including at least one Thy nucleobase have been prepared by extracting from ideal¹⁰⁰ or X-ray determined (1.6 Å resolution; PDB code 3BSE)¹⁰¹ B-DNA crystal structure and by saturating each broken chemical bond with a hydrogen atom. Geometry optimization is not performed for these simplified systems to avoid generating unattainable structure of normal DNA motions and no more solvent model is used. The prepared systems are shown in Figures 1 and S1. We investigate (1) environmental effect and (2) conformational effect; for (1) we study how the different environmental surroundings from B-DNA itself affect the Thy-related excitations of a core segment; for (2) we examine the variation of excitation properties of Thy-related excitations resulted from the geometry variation of a segment. For comparison, structures of dTpdT extracted from ideal and 3BSE source are also superimposed together in Figure S2.

Once these molecular systems are built, DFT/TDDFT calculations are carried out using Gaussian09¹⁰² with an economic basis set 6-31G(d)¹⁰³ since up to 100 excitations of a system as large as dApdTpdG will be computed in this work. However, the basis effect is also examined where 6-311+G(df,p)¹⁰⁴⁻¹⁰⁵ is tested, shown in Table S3, for a particular system – dTpdT. Moreover, since we focus on the solute form of the B-DNA molecule whose structure is stabilized ionizing one proton for each phosphate, extra electrons are added to each sliced B-DNA segment to account for the charged phosphates. For instance, dTpdT molecule, consisting of one phosphate, is set to have net charge $-e$. Therefore each molecule is a closed-shell electronic system and we pay attention to the singlet electronic excitations. Various exchange-correlation functionals – PBE1PBE¹⁰⁶, B3LYP¹⁰⁷⁻¹⁰⁸, CAM-B3LYP⁸², ω B97X⁸⁴, ω B97X-D⁸³ and LC- ω PBE⁸¹ – are implemented in the DFT/TDDFT calculations. After a TDDFT calculation, QNTO analysis is followed, whose code has been developed locally allowing us to process TDDFT output results generated by Gaussian09.

In the previous report⁹⁵ we have found TD- ω B97X among several tested theoretical methods most closely reproduce the transition origin of several low-lying excitations that EOM-

CCSD predicts for Thy and dT. Hence, dealing with larger DNA-sliced systems here, we focus on TD- ω B97X results; the results of TDDFT with other functionals are shown in Table S2.

3. Results and Discussion

3.1. The Excitation Energy, Oscillator Strength, and Transition Origin of Several Low-Lying Thy-related Excitations of Ideal di-Thy, 3BSE dT, Ideal/3BSE dTpdT--dApdA and Ideal/3BSE dApdTpdG

The detailed information of calculated absorption wavelength, oscillator strength and NTO1(2) transition origin of the first 10 selected Thy-related excitations of various systems are listed in Tables 1 and 2. Since we are interested in the influence of surrounding environment and conformational variation to Thy-related excitations, the standard-orbitals are chosen from the monomer orbitals of the ideal/3BSE Thy generated in its B3LYP-DFT calculations. The standard orbitals set can also be generated by other theoretical methods.

Incidentally, the orthogonality of DFT/B3LYP standard orbitals from different moiety of a DNA segment is maintained (mutual projection is below the accuracy, 10^{-2} , of the projection coefficients) for all the studied cases here. For cases where orthogonality is not fulfilled, such as the two moieties are very close to each other, the standard orbitals cannot be regarded as purely the monomer orbitals and orthogonalization has to be performed first.

Moreover, the targeted core – Thy – is rather intact within different situations studied here so that the Thy stays in the same chemical species, not other isomers with the same composition of atoms. Therefore, its ground state electronic structure remains the same. If the geometry of the target, Thy, is distorted strongly such that it, when let free, will be stabilized to other isomers, its ground state electronic structure is then changed, and the comparison of transition origins of two different species becomes meaningless. In such a case, the same set of standard-orbitals for electron from unoccupied orbitals and for hole from occupied orbitals also cannot be well defined, since some of the occupied and unoccupied orbitals can be switched. In Tables 1 and 2, the selected Thy-related excitations, denoted as SO-hosted (standard-orbitals hosted) excitations thereafter, are those with their hole-(NTO1-H) and electron-orbital (NTO1-E) of NTO1 having overall more than 30% density contribution from the standard-orbitals for hole and for electron, respectively. This is confirmed by first projecting the NTO1(2)-H(E) to the standard-orbitals and the density contribution of a standard-orbital is calculated by its square of projection coefficient. The panels a and b in Figure 2 show the standard-orbitals of the 2nd ideal Thy for hole and for electron, respectively. The other standard-orbitals of the 1st ideal, 1st 3BSE and 2nd 3BSE Thy for hole and for electron are similar to those in Figure 2. Therefore, for example, if the studied core molecular segment is the ideal di-Thy, the standard-orbitals used for projection of a NTO1(2)-H(E) will be the 6 orbitals of the 2nd ideal Thy shown in Figure 2 plus the other 6 similar orbitals from the 1st ideal Thy.

The detailed projection coefficients of the NTO1(2)-H(E) of each SO-hosted excitation are listed in Table S4. Moreover, the transition expression of a NTO1(2) is determined according to

Table 1 Various excitation properties of (a) ideal Thy, dT (adopted from Ref. 95), (b) ideal di-Thy, dTpdT, dTpdT--dApdA, and dApdTpdTpdG provided by TD- ω B97X calculation and QNTO analysis. N denotes excitation order, while P denotes NTO2 phase for cases where NTO1 has less than 70% domination to the whole excitation. λ (nm) and f stand for absorption wavelength and oscillator strength, respectively. NTO1(2) and % record the expression of transition origin of the first (second) NTO pair and its domination to the whole excitation. Type denotes the excitation classification based on the EOM-CCSD Thy NTO1 expressions used in Ref. 95. In (b) the excitation of a system is referenced to a similar excitation of the other ideal system shown in the subtitle (referred to as the core molecular unit). For instance, the 3rd excitation (Type-A2) of dTpdT is referenced to the 2nd excitation of di-Thy, while the 9th excitation (Type-E2B21) of dTpdT, having no similar type of excitation in di-Thy, is not referenced to any excitation. There is also data – Diff (%) of Energy, Diff(%) of f, and σ_E – recording the variation of energy, oscillator strength, and transition origin compared to the result of the referenced system. The local Type-A, B and C derived excitations are marked in bold-face font in the N column.

(a)

Ideal Thy						Ideal dT					
N	λ (nm)	f	NTO1	%	Type	N	λ (nm)	f	NTO1	%	Type
1	242.13	0.0002	N1t2 - S1t2	100	A2	1	239.80	0.0000	N1t2 - S1t2 (S2t2)	99	(A2)
2	228.82	0.2013	P1t2 - S1t2		B2	2	233.96	0.2820	P1t2 - S1t2	97	B2
3	190.78	0.0000	N1t2 N2t2 - (S1t2) S2t2	99	C2	3	190.28	0.0003	N1t2 N2t2 - (S1t2) S2t2	98	C2
4	178.49	0.0659	P2t2 - S1t2	99	D2	4	179.36	0.1967	P1t2 - S2t2	96	E2
5	174.43	0.1980	P1t2 - S2t2	98	E2	5	176.86	0.0825	P2t2 - S1t2	97	D2
6	164.14	0.0002	N2t2 - S1t2	97	F2	6	168.19	0.0015	N2t2 B (O) - S1t2	96	(F2)
7	158.49	0.0003	N1t2 N2t2 - (S1t2) S2t2	91	G2	7	159.11	0.0010	N1t2 N2t2 - (S1t2) S2t2	83	(G2)

(b)

N	λ (nm) ; Diff. (%) of Energy	f ; Diff. (%) of f	NTO1	σ_E	%	Type	N; P	λ (nm) ; Diff. (%) of Energy	f ; Diff. (%) of f	NTO1(2)	σ_E	%	Type				
Ideal di-Thy (ref. to ideal Thy)						Ideal dTpdT (ref. to ideal di-Thy)											
1	244.16	-1	0.0001	-	N1t1 - S1t1	0.017	99	A1	1	239.30	-3	0.0370	-70	P1t2 - S1t2	0.072	67	B2
2	242.42	0	0.0001	-	N1t2 - S1t2	0.020	99	A2	-	-	-	-	P1t1 - S1t1	-	30		
3	232.87	-2	0.1254	-38	P1t2 - S1t2	0.022	94	B2	2	236.23	-3	0.4157	90	P1t1 - S1t1	0.070	67	B1
4	228.92	0	0.2189	9	P1t1 - S1t1	0.044	94	B1	+	-	-	-	P1t2 - S1t2	-	30		
5	191.44	0	0	-	N1t2 N2t2 - (S1t2) S2t2	0.041	99	C2	3	235.97	3	0.0044	-	N1t2 - S1t2 (S2t2)	0.020	98	(A2)
6	190.81	0	0.0011	-	N1t1 N2t1 - (S1t1) S2t1	0.113	97	C1	4	235.06	4	0.0001	-	N1t1 - S1t1 (S2t1)	0.012	98	(A1)
7	188.49	-	0.0170	-	P1t1 - S1t2 (S2t1)	-	96	(E1B12)	6	192.01	-1	0.0001	-	N1t1 N2t1 - (S1t1) S2t1	0.030	96	C1
8	181.05	-1	0.0263	-60	P2t2 - S1t2	0.025	91	D2	7	189.63	-1	0.0292	72	P1t1 - S1t2 S2t1	0.049	94	E1B12
9	179.55	-	0.0568	-	P1t2 P2t1 - S1t1	-	84	D1B21	8	188.34	2	0.0037	-	N1t2 N2t2 - (S1t2) S2t2	0.044	95	C2
10	177.84	-	0.0749	-	P1t2 P2t1 - S1t1 (S2t2)	-	87	(D2E2B21)	9	186.74	-	0.0478	-	P1t2 B - S1t1 (S2t2)	-	88	(E2B21)
									10	185.94	-	0.0382	-	P1t2 B - S1t1	-	87	(B21)
									12	179.79	-	0.0912	-	P1t2 - S1t1 S2t2	-	92	E2B21
Ideal dTpdT--dApdA (ref. to ideal dTpdT)						Ideal dApdTpdTpdG (ref. to ideal dTpdT)											
1	242.05	-1	0.0383	4	P1t2 - S1t2	0.041	72	B2	1	242.97	-3	0.0480	-88	P1t1 - S1t1	0.106	78	B1
2	239.09	-1	0.4026	-3	P1t1 - S1t1	0.046	71	B1	2	239.62	0	0.2325	528	P1t2 - S1t2	0.100	76	B2
3	224.02	5	0.0001	-	N1t1 - S1t1 (S2t1)	0.018	96	(A1)	4	231.11	2	0.0001	-	N1t2 - S1t2 (S2t2)	0.024	94	(A2)
4	223.27	6	0.0001	-	N1t2 - S1t2 (S2t2)	0.029	96	(A2)	5	230.97	2	0.0001	-	N1t1 - S1t1 (S2t1)	0.010	93	(A1)
11	193.00	-1	0	-	(N1t1) N2t1 - (S1t1) S2t1	0.024	92	(C1)	15	194.60	-4	0.0363	-24	P1t2 - S1t1 (S2t2)	0.072	96	(E2B21)
16	189.76	-1	0.0001	-	(N1t2) N2t2 - (S1t2) S2t2	0.031	71	(C2)	16	192.01	-	0.0006	-	(N2t1) B - S1t1 (S2t1)	-	67	(F1)
17	188.97	-2	0.0209	-45	P1t2 - S1t1	0.095	92	(B21)	-	-	-	-	(N1t1) N2t1 B - (S1t1) S2t1	-	28		
19	186.79	2	0.0586	101	P1t1 - S1t2 (S2t1)	0.039	90	(E1B12)	18	190.91	1	0.0004	-	(N1t1) N2t1 B - S1t1 S2t1	0.163	59	(C1)
25	181.87	-	0.0042	-	P2t1 B - S1t1	-	83	(D1)	+	-	-	-	(N1t1) (N2t1) B - S1t1 S2t1	-	34		
26	180.96	-	0.0050	-	P2t2 A2 - S1t2	-	81	(D2)	21	188.45	1	0.0562	92	P1t1 - (S1t2) S2t1 (A)	0.122	80	(E1B12)
									24	186.62	1	0	-	N1t2 N2t2 - (S1t2) S2t2	0.031	93	C2
									28	182.31	-	0.0940	-	P1t2 - S2t2 (G)	-	68	(E2)
									+	-	-	-	P1t1 B - S1t2 (A) (G)	-	14		

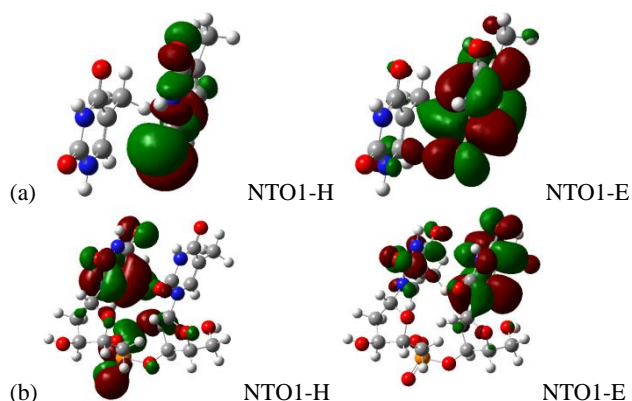


Fig. 3 Two examples of SO-hosted excitations of ideal di-Thy and dTpdT molecules. (a) The NTO1-H and NTO1-E plot for the 6th excitation (190.81nm, $f=0.0011$) of ideal di-Thy. NTO1 accounts for 97% of the whole excitation. With QNTO analysis the transition origin can be expressed in terms of standard-orbitals as “N1t1 N2t1 - (S1t1) S2t1”. (b) The NTO1 plot for the 9th excitation (186.74nm, $f=0.0478$) of ideal dTpdT. It accounts for 88% of the whole excitation and the transition origin reads “P1t2 B - S1t1 (S2t2)”.

these coefficients. To denote the transition expression, we introduce several notations: for example, P1t2 refers to P1 of the 2nd Thy with a positive coefficient in a system containing two Thys, e.g. di-Thy, dTpdT, while P1t₂ corresponds to P1 with a negative coefficient. P1t12 is an abbreviation of P1t1 plus P1t2 which both has density contribution greater than 0.3 in a NTO1(2)-H. Similarly, P1t12 corresponds to the case having combination of P1t1 and P1t2. In addition, the parenthesis “()” in P1t(1)2 indicates that it is made up of P1t1 and P1t2 but the coefficient of P1t1 is (0.3, 0.1].

The integration of the orbitals originated from backbone structure contributing to a NTO1(2)-H is denoted as B in a transition expression, whereas the integration of Thy orbitals other than the ones shown in the panels a and b in Figure 2 for NTO1(2)-H and for NTO1(2)-E, respectively, are both denoted as O. A1 and A2 are also likewise introduced for dTpdT--dApdA in a transition expression indicating the integrated contribution of orbitals from the 1st Ade and 2nd Ade, while A and G are introduced for dApdTpdTpdG indicating orbital-contribution from Ade and Gua. If the contribution of the orbital-fraction (B, O, A1, A2, A or G) is (0.3, 0.1], it is shown in “()” in the transi-

Table 2 Various excitation properties of the first 10 (8 for dT) SO-hosted singlet excitations of X-ray determined (3BSE) dT, dTpdT, dTpdT--dApdA and dApdTpdTpdG provided by TD- ω B97X calculation and QNTO analysis.

N; P	λ (nm); Diff. (%) of Energy	f; Diff. (%) of f	NT01(2)	σ_E	%	Type	N; P	λ (nm); Diff. (%) of Energy	f; Diff. (%) of f	NT01(2)	σ_E	%	Type				
3BSE dT (ref. to ideal dT)						3BSE dTpdT (ref. to ideal dTpdT)											
1	238.04	1	0.0005	-	N1 - S1 (S2)	0.018	99	(A)	1	238.34	-1	0.0001	-	N1t1 - S1t1	0.016	98	(A1)
2	228.90	2	0.2880	2	P1 - S1	0.016	97	B	2	235.85	0	0.0330	-92	P1t1(2) - S1t1(2)	0.221	56	(B1)
3	191.10	0	0.0015	-	N1 N2 - (S1) S2	0.026	98	C	-					P1t(1)2 (N1t2) - S1t(1)2		40	
4	176.81	0	0.0899	9	P2 - S1	0.021	91	D	3	234.90	0	0.0121	-	N1t2 - S1t2	0.023	87	(A2)
5	176.06	2	0.1881	-4	P1 - S2	0.021	89	E	4	231.25	3	0.4125	1015	P1t2 - S1t2	0.126	64	B2
6	168.14	0	0.0004	-	N2 B - S1	0.024	96	(F)	+					P1t1 - S1t1		32	
7	158.79	0	0.0037	-	(N1) N2 B (O) - S1 (S2)	-	72	(FG)	6	193.05	-1	0.0007	-	N1t1 N2t1 - (S1t1) S2t1	0.034	95	C1
8	157.45	-	0.0051	-	N1 B - S1 (S2)	-	57	(A')	8	190.86	-1	0.0013	-	N1t2 N2t2 - (S1t2) S2t2	0.030	91	C2
-					(N1) N2 (B) - (S1) S2		41		10	186.03	-	0.0045	-	P1t1 - S1t2	-	99	B12
									12	181.59	2	0.0363	-5	P1t2 - S1t1	0.137	96	B21
									13	178.62	-	0.0197	-	P1t1 - S2t1	-	53	E1
									-					(P1t2) P2t1 - S1t1 (S2t2)		29	
									14	177.66	-	0.0686	-	P2t1 - S1t1	-	46	D1
									+					P1t1 - (S1t2) S2t1			
3BSE dTpdT--dApdA (ref. to ideal dTpdT--dApdA)						3BSE dApdTpdTpdG (ref. to ideal dApdTpdTpdG)											
1	237.57	1	0.0755	-81	P1t1 - S1t1	0.069	74	B1	1	240.60	0	0.0494	-79	P1t2 - S1t2	0.065	81	B2
2	233.73	4	0.3469	806	P1t2 - S1t2	0.080	70	B2	3	234.53	4	0.2908	506	P1t1 - S1t1	0.063	75	B1
4	229.09	-2	0.0009	-	N1t1 - S1t1	0.015	83	A1	4	232.87	-1	0.0010	-	N1t2 O - S1t2	0.054	96	(A2)
5	226.27	-1	0.0032	-	N1t2 - S1t2 (S2t2)	0.031	95	(A2)	5	226.80	2	0.0001	-	N1t1 (O) - S1t1 (S2t1)	0.053	97	(A1)
13	193.23	0	0.0006	-	(N1t1) N2t1 - (S1t1) S2t1	0.047	96	(C1)	19	194.66	-4	0.0002	-	(N1t2) N2t2 (B) (O) - (S1t2) S2t2	0.068	86	(C2)
15	191.59	-1	0.0028	-	N1t2 N2t2 - (S1t2) S2t2	0.034	88	(C2)	23	190.65	0	0.0020	-	(N1t1) N2t1 (B) (O) - (S1t1) S2t1	0.101	82	(C1)
17	188.03	-	0.0089	-	P2t1 A1 (A2) - S1t1	0.061	75	(D1)	27	188.88	-	0.0167	-	P1t1 - S1t2	-	84	B12
19	186.87	2	0.0052	-51	P2t1 (A1) A2 - S1t1 (A1)	-	51	(D1')	32	183.95	-	0.0282	-	P1t1 - S2t1 G	-	83	(E1)
-					A1 - (S1t1) A1		27		37	182.17	-	0.0432	-	P1t2 (B) - S1t1	-	43	(B21)
20	185.89	-	0.0193	-	(P1t2) (P2t1) (A1) A2 - S1t1	-	52	(D1B 21)	+					B - G		37	
+					P2t(1)2 (A2) - S1t(1)2 (A1)		27		49	176.83	-	0.0922	-	P2t2 (B) - S1t2	-	59	(D2)
22	184.98	2	0.0261	25	P1t2 (B) - S1t1	0.082	83	(B21)	+					B - S1t1		16	

tion expression.

Following these rules, the transition expression of the excitations of each system can be determined. As an example, Figure 3 shows NTO1-H(E) of two excitations of di-Thy and dTpdT and the corresponding transition expressions. In addition, a similar categorization (Type-A~Type-G) introduced in the study of Thy and dT⁹⁵ for SO-hosted electronic excitations is also adopted here to classify electronic excitations: N1–S1 (Type-A); P1–S1 (Type-B); N1 N2–(S1) S2 (Type-C); P2–S1 (Type-D); P1–S2 (Type-E); N2–S1 (Type-F); N1 (N2)–S2 (Type-G). Since most of the studied segments here involve in two Thys, a SO-hosted excitation can be local (on the same Thy) or CT (across the two Thys) excitation. An excitation denoted as Type-A2 is therefore used to represent local Type-A excitation happened on the 2nd Thy. Type-B12, on the other hand, stands for a Type-B excitation with P1 orbital on the 1st Thy excited to the S1 orbital on the 2nd Thy. For simplicity, in the following discussions the terms “local Type-A(s)” will be used to refer to “local Type-A excitation(s)” and so on. Furthermore, an excitation can also be combined with different types of transitions. For instance, the excitation with NTO1 transition expression “P1t2 P2t1 - S1t1” is combined by Type-D1 local transition and Type-B21 CT transition with the opposite phase between P1t2 and P2t1 and is denoted as Type-D1B21.

We also employ σ_E (environmentally resulted root mean square deviation of standard-orbitals coefficients) for examining the environmental effect to NTO1 transition origins of excitations of a core molecular segment, while for comparing results of the same molecules extracted from ideal and 3BSE sources it is denoted as σ_G (geometry resulted deviation). The reference systems used for calculating different σ are detailed in Tables 1 and 2.

3.2. Ideal Thy vs. di-Thy

To detail the environmentally resulted variation of excitation properties of several chosen core segments consisting of Thy(s), we take a deeper look into each type of electronic excitations. We first compare the results of ideal Thy and di-Thy shown in Table 1.

Local Type-B

Obviously the single bright local Type-B of Thy at 228.82nm evolves into two bright excitations of di-Thy: one being a little weakened at 232.87nm (Type-B2) and the other a little enhanced at 228.92nm (Type-B1). Moreover, the two bright excitations of di-Thy are both dominated by single NTO1 instead of by two similar weighted local transitions given in molecular exciton theory⁹⁸. Therefore the separation of the two Thys is short such that their interaction cannot be well described by dipole-dipole interaction.

Local Type-A/C

As for the local Type-A, its absorption wavelength of Thy at 242.13nm results in the Type-A1 and Type-A2 of di-Thy at 244.16nm and 242.42nm; in other words, almost no energy splitting occurs. This is attributed to the weak transition dipole of Thy, which also leads to the small oscillator strengths. Similarly, no energy splitting occurs for the two weak local Type-C absorptions as well.

Local Type-D/E; CT Type-B

For even higher-lying excitations, Table 1(b) shows that they are mainly formed by local Type-D/E and CT Type-B transitions. The local Type-D/E involved excitations, like local Type-Bs mentioned above, have one brighter and the other darker and are both dominated by single NTO1. Moreover, their oscillator strengths are weakened by the mixture of CT Type-B transition. We can see that, for example, the brighter excitation involved with local Type-D transition of di-Thy at 179.55nm (Type-D1B21, $f=0.0568$) is still weaker than the pure Type-D of Thy at 178.49nm ($f=0.0659$).

The σ_E for each local excitation shows that the Type-C1 of di-Thy has the largest deviation to be 0.113, but its transition expression feature remains intact.

3.3. Ideal di-Thy vs. dTpdT

We now move onto the effect of link between two Thys, i.e. the DNA backbone, on electronic excitations.

Local Type-B

In the presence of DNA backbone, the two bright absorption peaks of di-Thy become a brighter one and a darker one of dTpdT. The stronger one is predicted to be a Type-B1 (and with NTO2 “P1t2 - S1t2”) at 236.23nm while the weaker one is a Type-B2 (with NTO2 “P1t1 - S1t1”) at 239.30nm. Moreover, they both have a 3% energy lowering. Therefore it clearly shows that the presence of backbone is significant to modify the NTO1 transition origin of two original local Type-Bs of di-Thy, even if it does not donate orbitals to NTO1(2)-H(E). We find that the backbone here promotes the formation of exciton-like excitations only present for larger distance of two Thys, that is, $\frac{1}{\sqrt{2}}(\varphi_u^* \varphi_v \pm \varphi_u \varphi_v^*)$, where φ_u^* and φ_u is the excited and unexcited wavefunctions of monomer u and φ_v^* and φ_v those of monomer v of a dimer system composed of two geometrically identical monomers.

Local Type-A/C

Next we deal with the local Type-A. In the presence of backbone the two local Type-As instead have 3% and 4% energy arising, in contrast to the energy-lowering imposed on the local Type-Bs discussed above. The energy arising and lowering result in excitation reordering such that the lowest singlet excitation (Singlet-1) changes from a local Type-A to a local Type-B. Therefore, although still not taking into account more factors yet, e.g. base stacking, WC pairing nucleobases, ions, solvent molecules etc., the addition of backbone to di-Thy readily changes the excitation of Singlet-1. The presence of backbone also results in a slight S2-component mixing into the Type-A1 and Type-A2.

The remaining two ¹nπ*-character excitations of di-Thy, i.e. local Type-Cs, though switching their relative order, retain their main feature of absorption energy, oscillator strength and transition origin of NTO1 in the presence of backbone.

Local Type-D/E; CT Type-B

Finally we consider the excitations formed by the mixture of CT Type-B transition and local Type-D/E transition. The Type-E1B12 has a strong enhancement of 72% of oscillator strength (from 0.0170 to 0.0292) with a small shifted excitation energy (188.49nm to 189.63nm), while the excitations of di-Thy with local Type-D transition (181.05nm, 179.55nm and 177.84nm)

disappear in all the listed SO-excitations of dTpdT. Instead, they are replaced by excitations with local Type-E and/or CT Type-B transitions; that is, 186.74nm, 185.94nm and 179.79nm absorptions of dTpdT. Furthermore, the backbone orbital component is strongly involved in the 186.74nm and 185.94nm excitations. These results suggest that the larger average distance of electron transition which encompasses wider spatial area for these higher-lying excitations results in the high backbone-sensitivity.

3.4. Ideal dTpdT vs. dTpdT--dApdA

Local Type-B

For even larger system with dApdA in the opposing strand in charge of WC hydrogen bonding effect, the TD- ω B97X calculated absorption spectrum (Figure S3) shows that there are two strong peaks. However, after examining their NTO1 transition origins only the lower energy one at 239.09nm corresponds to a SO-hosted (Type-B1) excitation. Its NTO1 transition origin is very similar to that of the brightest peak of dTpdT and it has a minor energy shift (-1%). A similar situation also happens to the weaker Type-B2, the Singlet-1.

Local Type-A/C

The NTO1 transition origins of the two local Type-As are retained as well, but again their excitation energies arise (5% and 6%). For the two local Type-Cs, their absorption energies have minor deviation accompanied with a modest σ_E (0.024 and 0.031).

Local Type-D/E; CT Type-B

For the CT Type-B involved excitations, interestingly the mixed local Type-E transition appearing in the result of dTpdT diminishes as dApdA is in effect, and two local Type-E involved excitations of dTpdT (186.74nm and 179.79nm) are replaced by local Type-D involved ones of dTpdT--dApdA (181.87nm and 180.96nm). The 180.96nm excitation even mixes in A2 in its transition expression. The remaining Type-E1B12 also has a quite large increase (101%) in its oscillator strength even if its absorption energy is rather intact. Therefore again environment effect is more pronounced in these higher-lying excitations.

3.5. Ideal dTpdT vs. dApdTpdTpdG

Local Type-B

In the presence of stacking nucleobases next to dTpdT and the backbone linking them, i.e. dApdTpdTpdG, the two local Type-Bs switch their positions such that the brighter absorption changes from the Type-B1 to the Type-B2, even if their excitation energies are not modified much. The oscillator strength of the brighter one is also dampened one half, while that of the darker one is enhanced. Hence it can be concluded that the local Type-Bs are quite sensitive to environmental surroundings of backbone and stacking nucleobases. They can be more exciton-like excitations, or can be well separated like two local ones. This can be comprehended that the environments experienced by the two Thys can mediate the degree of near-degeneracy of their local transitions so that the formation of exciton-like excitations can be tuned.

Local Type-A/C

On the other hand, the two local Type-As again have a 2% energy arising and a minor change of transition origin compared to the results of dTpdT.

As for the two local Type-Cs, the Type-C2 seems to be unspoiled in its transition origin but Type-C1 is strongly contaminated with backbone-orbital, also reflected in its large σ_E (0.163); its NTO1 domination also decreases substantially. However, the energies of the two excitations are both rather intact.

Local Type-D/E; CT Type-B

The remaining excitations related to local Type-E and/or CT Type-B transitions of dTpdT again are affected quite intensively. The Type-E1B12, although retains similar excitation energy, have almost doubled its oscillator strength and its NTO1 transition expression mixes in A with S1t2 being diminished at the same time. On the other hand, the Type-E2B21 has more notable energy lowering (4%) but oscillator strength reduction (24%). The remaining Type-B21 and Type-E2B21 of dTpdT are replaced by the Type-F1 and Type-E2, both of which have noticeable other components, e.g. B, A or G, mixed in the transition expressions.

Therefore, the bases-stacking influence appears more pronounced than that of WC-pairing nucleobases through hydrogen bonding, as it leads to averagely larger σ_E .

3.6. Ideal vs. 3BSE (X-ray crystal) structures

We examine the effect of conformation variation on electronic excitation properties of dT, dTpdT, dTpdT--dApdA and dApdTpdTpdG. The transition origins of excitations of geometrically different systems can be compared with each other, given that the segment stays in the chemically same species.

dT

The detailed information of the first 10 (8 for dT) SO-hosted excitation of each 3BSE system is listed in Table 2. We can observe that for dT all 8 SO-hosted excitations except for the highest-lying Type-G can be well traced. A one-to-one mapping can then be readily made from their NTO1 transition origin. Moreover, their absorption energies, oscillator strengths and NTO1 transition origins are largely retained.

dTpdT

Analysis on dTpdT shows that the conformation variation is quite influential to the NTO1 transition origin of the two local Type-Bs such that the σ_G value for Type-B1 is 0.221 and for Type-B2 is 0.126. The stronger absorption also transforms from the Type-B1 to the Type-B2, even if energy and oscillator strength of the stronger and weaker are modified little.

In contrast, the local Type-As and Type-Cs are rather sustainable in the NTO1 transition origin and absorption energy to conformation change, and their oscillator strengths remain small. Moreover, the Singlet-1 becomes Type-A1.

The remaining listed higher-lying excitations have rather large variations in their NTO1 transition origin although they are still around the absorption wavelength of 170nm~190nm; this can also be observed in the results of ideal di-Thy, dTpdT, dTpdT--dApdA and dApdTpdTpdG, that is, CT Type-B involved excitations are all located in this energy range, though their composition of NTO1 transition origin is very sensitive to the surrounding environment.

dTpdT--dApdA and dApdTpdTpdG

For much larger systems dTpdT--dApdA and dApdTpdTpdG, one may expect that conformation change accumulation should

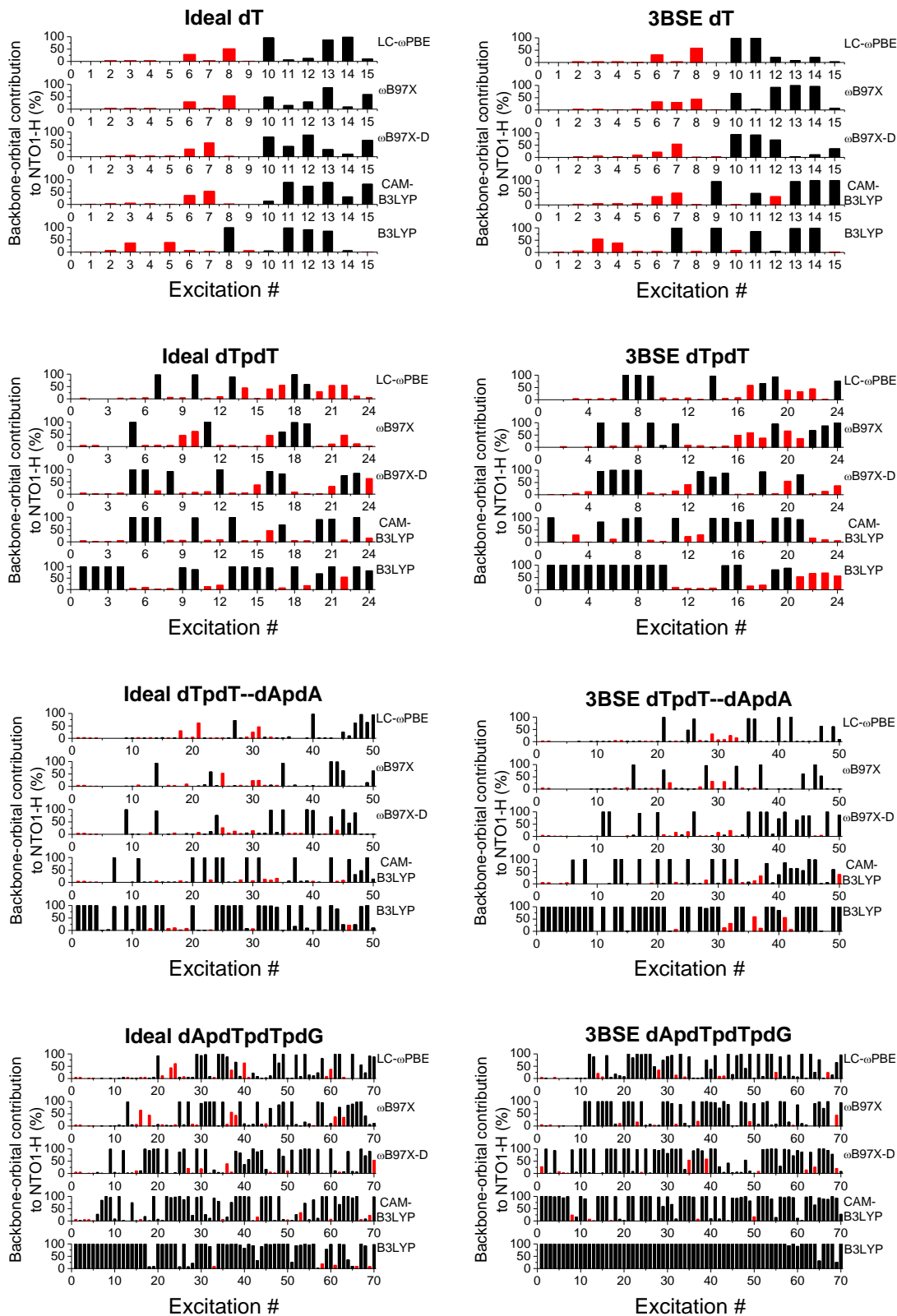


Fig. 4 Percentage of backbone density contribution to the NTO1-H of the first several excitations of the backbone-included systems. Red columns indicate SO-hosted excitations.

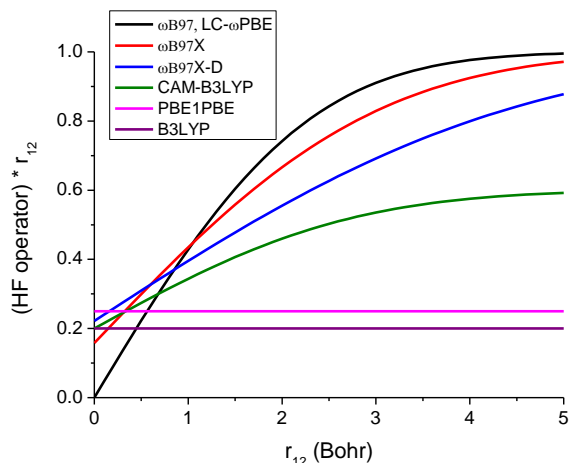


Fig. 5 $L(r_{12})$ vs. r_{12} for different functionals. For details, please see the text and Eqs. (1) ~ (3).

lead to quite distinct excitation properties. This seems to be the case for dApdTpdTpdG as only 6 excitations out of 10 can better correspond to excitations found in the result of ideal structure. Moreover, mixture of orbitals other than the standard-orbitals to transition origin often occurs. For example, Type-C1 and -C2 both have B and O involved in the transition expressions such that the ratio of local Type-C Thy-orbitals contributing to the total electronic density reduces. On the other hand, for dTpdT--dApdA there remains many excitations that can be well traced for the local Type-A, B and C transitions; the brighter and weaker local Type-Bs again exchange their NTO1 transition origin which should be due to their sensitivity to the coupling of the two Thys⁹⁷.

Overall, it can be seen that conformation influence can be the same or even outstrip environmental effects to the excitation properties of the SO-hosted excitations.

3.7. Detailed Backbone-Orbital Involvement in the First Several Excitations of B-DNA Segments Containing Backbone

Figure 4 shows the percentage of backbone-orbital density contributing to NTO1-H in the first 15, 24, 50, and 70 excitations (not only SO-hosted ones) of dT, dTpdT, dTpdT--dApdA, and dApdTpdTpdG, respectively. TD-B3LYP underestimates the absorption energy of a lot of backbone-to-base excitations crowding around the first several excitations. However, even LC hybrid functionals predict an impressive involvement of backbone-orbital in several excitations.

As shown in Eq. (2), the $L(r_{12})$ in a LC hybrid functional can be interpreted as a r_{12} -dependent proportion of HF exchange. For example, both ω B97 and LC- ω PBE adopt $L(r_{12}) = \text{erf}(\omega r_{12})$, with $\omega = 0.4 \text{ Bohr}^{-1}$, while ω B97X adopts $L(r_{12}) = a_x \times [1 - \text{erf}(\omega r_{12})] + \text{erf}(\omega r_{12})$, with $\omega = 0.3 \text{ Bohr}^{-1}$ and $a_x = 0.157706$. By contrast, a global hybrid functional, containing a fixed proportion c_x of HF exchange, adopts $L(r_{12}) = a_x$ and a pure DFA, containing no HF exchange, adopts $L(r_{12}) = 0$.

To look into more details, we plot, in Figure 5, the r_{12} -dependent proportion of Hartree-Fock exchange $L(r_{12})$, for various functionals. Evidently we observe that there is a strong correlation between the prescribed HF-exchange fraction in a LC hybrid functional and the appearance of significant backbone-to-base CT contributions to excitations. As the $L(r_{12})$ is larger for a functional in the range of inter-electronic separation $r_{12} > 1 \text{ Bohr}$ for the electron-hole interaction, the first excitation that has a significant contribution from backbone to NTO1-H appears earlier.

The growing up diversities among the results given by different LC hybrid functionals calculations (CAM-B3LYP⁸², ω B97X⁸⁴, ω B97X-D⁸³ and LC- ω PBE⁸¹) due to the increase in the molecular size (dTpdT, dTpdT--dApdA, dApdTpdTpdG) suggest that the description of excitation order and transition origins is quite sensitive to the prescription of $L(r_{12})$ for larger and more complex systems. Therefore, finer tunings and revisions to the currently used functionals are necessary in order to achieve a more consistent description of these larger electronic systems for which more benchmarks are in need. Nevertheless, up to this point, we could still conclude that the DNA backbone is quantum mechanically quite important that its orbitals contribution is often strongly involved in the h-orbital of the electronic excitations of B-DNA.

4. Conclusion

We have examined several low-lying electronic excitations of various Thy-contained systems extracted from two sources of B-DNA, i.e. the ideal and a X-ray crystal structure. Various environmental and conformational effects on Thy-related excitations have been investigated quantum mechanically. The later and former effects are studied by comparing the LC-TDDFT results of two systems that are different from each other in geometry and in a physical/chemical surrounding, respectively. Through the employment of QNTO analysis, the transition origin of up to hundred electronic excitations of different systems can readily be determined and therefore similar excitations can be identified and compared with each other.

We find that although many low-lying SO-hosted $^1\pi\pi^*$ - and $^1n\pi^*$ -character excitations (or combinations of them) of Thy-contained systems can be interpreted by single NTO1, there are still several cases that NTO1 has less than 70% domination, in which case NTO2 is also taken into account. Therefore the present study provides a more realistic description of molecular exciton view in which the contribution of the local electronic transitions proportion can be different. Moreover, decomposition of NTO1(2)-H(E) of an excitation into standard-orbitals helps pinpoint its transition origin. It is possible that an excitation is a mixture of different local and CT transitions. It is also found that as the segment size grows to include in backbone or WC-pairing or adjacent stacking nucleobases, the NTO1 transition origin is often more complicated because various orbital-components are mixed; the NTO1 domination is also likely to decrease at the same time. Our analysis provides a quantitative investigation foundation for these complex phenomena.

Furthermore, both conformational and environmental effects to SO-hosted excitations are found to mediate not only the absorption energy and oscillator strength but also the NTO1

transition origin. This situation is significant especially for the higher-lying excitations composed of CT transitions. It is found that the higher-lying local Type-D, E and CT Type-B transitions are more sensitive to environmental surroundings as well as conformation variations than local Type-A, B and C transitions such that they often bear various mixtures to form the transition origin of excitations around 170nm~190nm. This situation probably results from their near-degenerate feature of transitions.

Overall, the present study suggests that a DNA molecule continually under various interactions with itself or environmental molecules in solution can exhibit from time to time a slightly or very different transition origin of NTO1(2) depending on its experience at the instance of light-absorptions. It has also been reviewed in the Chap. 14 of Ref. 36 that various electronic properties of nucleobases are notably dependent on their microscopic environment and present QNTO analysis helps further provide a systematic quantum chemistry framework to investigate them. Moreover, the origins of two electronic excitations of the same or different systems can be, as expressed by standard-orbitals, quite different even if their absorption energy and oscillator strength are similar to each other, which implies that a further determination of correct transition origin of an excitation is quite important which governs later dynamics of an electronically excited molecule.

Other possible effects such as solvents which are not considered in the present work are anticipated to be applicable in QNTO framework as well. The present scheme can also be readily extended to construct the potential energy surface of a gradually geometrically modified system within a complex environment because an electronic excited state can be well traced from its transition origin. More applications are underway.

Acknowledgements

We would like to thank National Science Council (NSC), and National Center of Theoretical Sciences (NCTS) for their financial supports. We would also like to thank National Center for High-performance Computing (NCHC) for providing computational resources.

References

- (1) D. L. Nelson and M. M. Cox, *Lehninger Principles of Biochemistry*, W. H. Freeman & Company, New York, 3rd edn, 2000.
- (2) R. F. Weaver, *Molecular Biology*, McGraw-Hill, New York, 4th edn, 2007.
- (3) P. W. Rothemund, *Nature*, 2006, **440**, 297.
- (4) E. S. Andersen, M. Dong and M. M. Nielsen, *Nature*, 2009, **459** (7243), 73.
- (5) Y. Ishitsuka and T. Ha, *Nat. Nanotechnol.*, 2009, **4**, 281.
- (6) F. A. Aldaye, A. L. Palmer and H. F. Sleiman, *Science*, 2008, **321**, 1795.
- (7) C. E. Crespo-Hernandez, B. Cohen, P. M. Hare and B. Kohler, *Chem. Rev.*, 2004, **104**, 1977.
- (8) M. K. Shukla and J. Leszczynski, *J. Biomol. Struct. Dyn.*, 2007, **25**, 93.
- (9) T. Inagaki, A. Ito, K. Heida and T. Ho, *Photochem. Photobiol.*, 1986, **44**, 303.
- (10) J. S. Novros and L. B. Clark, *J. Phys. Chem.*, 1986, **90**, 5666.

- (11) Y. Matsuoka and B. Norden, *J. Phys. Chem.*, 1982, **86**, 1378.
- (12) A. Holmen, A. Broo and B. Albinsson, *J. Phys. Chem.*, 1994, **98**, 4998.
- (13) E. Nir, C. Janzen, P. Imhof, K. Kleineremanns and M. S. de Vries, *J. Chem. Phys.*, 2001, **115**, 4604.
- (14) M. Mons, I. Dimicoli, F. Piuze, B. Tardivel and M. Elhanine, *J. Phys. Chem. A*, 2002, **106**, 5088.
- (15) M. Mons, F. Piuze, I. Dimicoli, L. Gorb and J. Leszczynski, *J. Phys. Chem. A*, 2006, **110**, 10921.
- (16) M. K. Shukla and J. Leszczynski, *Chem. Phys. Lett.*, 2006, **429**, 261.
- (17) C. A. Sprecher and W. C. Johnson Jr., *Biopolymers*, 1977, **16**, 2243.
- (18) L. B. Clark, *J. Am. Chem. Soc.*, 1977, **99**, 3934.
- (19) L. B. Clark, *J. Am. Chem. Soc.*, 1994, **116**, 5265.
- (20) C. Santhosh and P. C. Mishra, *J. Mol. Struct.*, 1989, **198**, 327.
- (21) D. W. Miles, S. J. Hann, R. K. Robins and H. Eyring, *J. Phys. Chem.*, 1968, **72**, 1483.
- (22) L. B. Clark, *J. Phys. Chem.*, 1989, **93**, 5345.
- (23) L. B. Clark, *J. Phys. Chem.*, 1990, **94**, 2873.
- (24) A. Holmen, A. Broo, B. Albinsson and B. Norden, *J. Am. Chem. Soc.*, 1997, **119**, 12240.
- (25) L. B. Clark, *J. Phys. Chem.*, 1995, **99**, 4466.
- (26) N. J. Kim, G. Jeong, Y. S. Kim, J. Sung, S. K. Kim and Y. D. Park, *J. Chem. Phys.*, 2000, **113**, 10051.
- (27) D. C. Luhrs, J. Viallon and I. Fischer, *Phys. Chem. Chem. Phys.*, 2001, **3**, 1827.
- (28) E. Nir, K. Kleineremanns, L. Grace and M. S. de Vries, *J. Phys. Chem. A*, 2001, **105**, 5106.
- (29) D. Voet, W. B. Gratzer, R. A. Cox and P. Doty, *Biopolymers*, 1963, **1**, 193.
- (30) L. B. Clark and I. Tinoco Jr., *J. Am. Chem. Soc.*, 1965, **87**, 11.
- (31) T. Yamada and H. Fukutome, *Biopolymers*, 1968, **6**, 43.
- (32) F. Zaloudek, J. S. Novros and L. B. Clark, *J. Am. Chem. Soc.*, 1985, **107**, 7344.
- (33) W. C. Johnson Jr., P. M. Vipond and J. C. Girod, *Biopolymers*, 1971, **10**, 923.
- (34) A. Kaito, M. Hatano, T. Ueda and S. Shibuya, *Bull. Chem. Soc. Jpn.*, 1980, **53**, 3073.
- (35) K. Raksany and I. Foldvary, *Biopolymers*, 1978, **17**, 887.
- (36) *Radiation Induced Molecular Phenomena in Nucleic Acids*, ed. M. K. Shukla and J. Leszczynski, Springer-Verlag, 2008.
- (37) M. K. Shukla and J. Leszczynski, *Computational Chemistry: Reviews of Current Trends, vol 8.*, ed. J. Leszczynski, World Scientific, Singapore, 2003, p. 249.
- (38) B. Mennucci, A. Toniolo and J. Tomasi, *J. Phys. Chem. A*, 2001, **105**, 4749.
- (39) M. K. Shukla and P. C. Mishra, *Chem. Phys.*, 1999, **240**, 319.
- (40) M. K. Shukla, S. K. Mishra, A. Kumar and P. C. Mishra, *J. Comput. Chem.*, 2000, **21**, 826.
- (41) S. K. Mishra, M. K. Shukla and P. C. Mishra, *Spectrochim. Acta. Part. A*, 2000, **56**, 1355.
- (42) A. Broo, *J. Phys. Chem. A*, 1998, **102**, 526.
- (43) M. K. Shukla and J. Leszczynski, *J. Phys. Chem. A*, 2002, **106**, 11338.

- (44) M. P. Fulscher, L. Serrano-Andres and B. O. Roos, *J. Am. Chem. Soc.*, 1997, **119**, 6168.
- (45) J. Lorentzon, M. P. Fulscher and B. O. Roos, *J. Am. Chem. Soc.*, 1995, **117**, 9265.
- (46) M. P. Fulscher and B. O. Roos, *J. Am. Chem. Soc.*, 1995, **117**, 2089.
- (47) T. Fleig, S. Knecht and C. Hattig, *J. Phys. Chem. A*, 2007, **111**, 5482.
- (48) H. H. Ritze, P. Hobza and D. Nachtigallova, *Phys. Chem. Chem. Phys.*, 2007, **9**, 1672.
- (49) B. Mennucci, A. Toniolo and J. Tomasi, *J. Phys. Chem. A*, 2001, **105**, 4749.
- (50) Mennucci, B.; Toniolo, A.; Tomasi, J. *J. Phys. Chem. A* **2001**, 105, 7126-7134.
- (51) M. K. Shukla and J. Leszczynski, *J. Comput. Chem.*, 2004, **25**, 768.
- (52) A. Tsolakidis and E. Kaxiras, *J. Phys. Chem. A*, 2005, **109**, 2373.
- (53) D. Varsano, R. D. Felice, M. A. L. Marques and A. Rubio, *J. Phys. Chem. B*, 2006, **110**, 7129.
- (54) J. Cerny, V. Spirko, M. Mons, P. Hobza and D. Nachtigallova, *Phys. Chem. Chem. Phys.*, 2006, **8**, 3059.
- (55) R. Improta and V. Barone, *J. Am. Chem. Soc.*, 2004, **126**, 14320.
- (56) T. Gustavsson, A. Banyasz, E. Lazzarotto, D. Markovitsi, G. Scalmani, M. J. Frisch, V. Barone and R. Improta, *J. Am. Chem. Soc.*, 2006, **128**, 607.
- (57) R. So and S. Alavi, *J. Comput. Chem.*, 2007, **28**, 1776.
- (58) R. J. Bartlett and M. Musial, *Rev. Mod. Phys.*, 2007, **79**, 291.
- (59) H. Sekino and R. J. Bartlett, *Int. J. Quantum Chem. Symp.*, 1984, **18**, 255.
- (60) J. F. Stanton and R. J. Bartlett, *J. Chem. Phys.*, 1993, **98**, 7029.
- (61) E. Runge and E. K. U. Gross, *Phys. Rev. Lett.*, 1984, **52**, 997.
- (62) *Time-Dependent Density-Functional Theory*, ed. M. A. L. Marques, C. A. Ullrich, F. Nogueira, A. Rubio, K. Burke and E. K. U. Gross, Springer-Verlag, 2006.
- (63) M. E. Casida, in *Recent Advances in Density Functional Methods, vol. 1*, ed. D. P. Chong, World Scientific, Singapore, 1995.
- (64) A. Dreuw and M. Head-Gordon, *Chem. Rev.*, 2005, **105**, 4009.
- (65) J. Neugebauer, *J. Phys. Chem. B*, 2008, **112**, 2207.
- (66) J. Neugebauer, *J. Chem. Phys.*, 2007, **126**, 134116.
- (67) M. Dulak, J. W. Kamiński and T. A. Wesolowski, *J. Chem. Theory Comput.*, 2007, **3**, 735.
- (68) J. W. Kaminski, S. Gusarov, T. A. Wesolowski and A. Kovalenko, *J. Phys. Chem. A*, 2010, **114**, 6082.
- (69) M. Dulak, J. W. Kamiński and T. A. Wesolowski, *Int. J. Quantum Chem.*, 2009, **109**, 1886.
- (70) A. W. Götz, S. M. Beyhan and L. Visscher, *J. Chem. Theory Comput.*, 2009, **5**, 3161.
- (71) J. Neugebauer, *J. Chem. Phys.*, 2009, **131**, 084104.
- (72) S. Fux, C. R. Jacob, J. Neugebauer, L. Visscher and M. Reiher, *J. Chem. Phys.*, 2010, **132**, 164101.
- (73) K. Kiewisch, G. Eickerling, M. Reiher and J. Neugebauer, *J. Chem. Phys.*, 2008, **128**, 044114.
- (74) J. Neugebauer, *ChemPhysChem*, 2009, **10**, 3148.
- (75) J. Neugebauer, C. Curutchet, A. Muñoz-Losa and B. Mennucci, *J. Chem. Theory Comput.*, 2010, **6**, 1843.
- (76) C. R. Jacob and L. Visscher, *J. Chem. Phys.*, 2008, **128**, 155102.
- (77) T. A. Wesolowski, *J. Am. Chem. Soc.*, 2004, **126**, 11444.
- (78) G. Fradelos, J. W. Kaminski, T. A. Wesolowski and S. Leutwyler, *J. Phys. Chem. A*, 2009, **113**, 9766.
- (79) C. R. Jacob, J. Neugebauer and L. Visscher, *J. Comput. Chem.*, 2008, **29**, 1011.
- (80) J. Neugebauer, *Physics Reports*, 2010, **489**, 1.
- (81) O. A. Vydrov, J. Heyd, A. V. Kruckau and G. E. Scuseria, *J. Chem. Phys.*, 2006, **125**, 074106.
- (82) T. Yanai, D. Tew and N. Handy, *Chem. Phys. Lett.*, 2004, **393**, 51.
- (83) J.-D. Chai and M. Head-Gordon, *Phys. Chem. Chem. Phys.*, 2008, **10**, 6615.
- (84) J.-D. Chai and M. Head-Gordon, *J. Chem. Phys.*, 2008, **128**, 084106.
- (85) J.-D. Chai and M. Head-Gordon, *Chem. Phys. Lett.*, 2008, **467**, 176.
- (86) J.-D. Chai and M. Head-Gordon, *J. Chem. Phys.*, 2009, **131**, 174105.
- (87) A. Savin, in *Recent Developments and Applications of Modern Density Functional Theory*, ed. J. M. Seminario, Elsevier, Amsterdam, 1996, p. 327.
- (88) H. Iikura, T. Tsuneda, T. Yanai and K. Hirao, *J. Chem. Phys.*, 2001, **115**, 3540.
- (89) Y. Tawada, T. Tsuneda, S. Yanagisawa, T. Yanai and K. Hirao, *J. Chem. Phys.*, 2004, **120**, 8425.
- (90) J. A. Parkhill, J.-D. Chai, A. D. Dutoi and M. Head-Gordon, *Chem. Phys. Lett.*, 2009, **478**, 283.
- (91) J.-W. Song, T. Hirose, T. Tsuneda and K. Hirao, *J. Chem. Phys.*, 2007, **126**, 154105.
- (92) M. A. Rohrdanz and J. M. Herbert, *J. Chem. Phys.*, 2008, **129**, 034107.
- (93) D. Jacquemin, E. A. Perpète, I. Ciofini and C. Adamo, *Theor. Chem. Acc.*, 2011, **128**, 127.
- (94) M. Caricato, G. W. Trucks, M. J. Frisch and K. B. Wiberg, *J. Chem. Theory Comput.*, 2011, **7**, 456.
- (95) J.-H. Li, J.-D. Chai, G. Y. Guo and M. Hayashi, *Chem. Phys. Lett.*, 2011, **514**, 362.
- (96) A. G. Leslie, S. Arnott, R. Chandrasekaran and R. L. Ratliff, *J. Mol. Biol.*, 1980, **143**, 49.
- (97) C. R. Kozak, K. A. Kistler, Z. Lu and S. Matsika, *J. Phys. Chem. B*, 2010, **114**, 1674.
- (98) M. Kasha, *Radiat. Res.*, 1963, **20**, 55.
- (99) A. W. Lange and J. M. Herbert, *J. Am. Chem. Soc.*, 2009, **131**, 3913.
- (100) Ideal B-DNA PDB file adopted from "http://www.biochem.umd.edu/biochem/kahn/teach_res/dna_tutorial/".
- (101) N. Narayana and M. A. Weiss, *J. Mol. Biol.*, 2009, **385**, 469.
- (102) M. J. Frisch, G. W. Trucks, H. B. Schlegel, G. E. Scuseria, M. A. Robb, J. R. Cheeseman, G. Scalmani, V. Barone, B. Mennucci, G. A. Petersson, H. Nakatsuji, M. Caricato, X. Li, H. P. Hratchian, A. F. Izmaylov, J. Bloino, G. Zheng, J. L. Sonnenberg, M. Hada, M. Ehara, K. Toyota, R. Fukuda, J. Hasegawa, M. Ishida, T. Nakajima, Y. Honda, O. Kitao, H. Nakai,

-
- T. Vreven, J. A. Montgomery, Jr., J. E. Peralta, F. Ogliaro, M. Bearpark, J. J. Heyd, E. Brothers, K. N. Kudin, V. N. Staroverov, R. Kobayashi, J. Normand, K. Raghavachari, A. Rendell, J. C. Burant, S. S. Iyengar, J. Tomasi, M. Cossi, N. Rega, J. M. Millam, M. Klene, J. E. Knox, J. B. Cross, V. Bakken, C. Adamo, J. Jaramillo, R. Gomperts, R. E. Stratmann, O. Yazyev, A. J. Austin, R. Cammi, C. Pomelli, J. W. Ochterski, R. L. Martin, K. Morokuma, V. G. Zakrzewski, G. A. Voth, P. Salvador, J. J. Dannenberg, S. Dapprich, A. D. Daniels, Ö. Farkas, J. B. Foresman, J. V. Ortiz, J. Cioslowski and D. J. Fox, Gaussian 09, Revision A.1, Gaussian, Inc., Wallingford CT, 2009.
- (103) R. Ditchfield, W. J. Hehre and J. A. Pople, *J. Chem. Phys.*, 1971, **54**, 724.
- (104) A. D. McLean and G. S. Chandler, *J. Chem. Phys.*, 1980, **72**, 5639.
- (105) R. Krishnan, J. S. Binkley, R. Seeger and J. A. Pople, *J. Chem. Phys.*, 1980, **72**, 650.
- (106) C. Adamo and V. Barone, *J. Chem. Phys.*, 1999, **110**, 6158.
- (107) A. D. Becke, *J. Chem. Phys.*, 1993, **98**, 5648.
- (108) C. Lee, W. Yang and R. G. Parr, *Phys. Rev. B*, 1988, **37**, 785.

Supporting Information

Significant Role of DNA Backbone in Mediating the Transition Origin of Electronic Excitations of B-DNA – Implication from Long Range Corrected TDDFT and Quantified NTO Analysis

Jian-Hao Li^{a, b}, Jeng-Da Chai^{a, c, *}, Guang-Yu Guo^{a, c, d}, Michitoshi Hayashi^{b, *}

^aDepartment of Physics, Center for Theoretical Sciences, National Taiwan University, Taipei, 10617, Taiwan

^bCenter for Condensed Matter Sciences, National Taiwan University, Taipei, 10617, Taiwan

^cCenter for Quantum Science and Engineering, National Taiwan University, Taipei, 10617, Taiwan

^dGraduate Institute of Applied Physics, National Chengchi University, Taipei 11605, Taiwan

E-mail: jdchai@phys.ntu.edu.tw (J.-D. Chai); atmyh@ntu.edu.tw (M. Hayashi)

Contents

1.	Table S1 for the major internal coordinates of DNA backbone of ideal and 3BSE dTpdT.	S2
2.	Table S2 for the excitation properties of ideal B-DNA segments calculated by TDDFT with global hybrid (B3LYP and PBE1PBE) and LC hybrid (CAM-B3LYP, ω B97X-D, and LC- ω PBE) functionals other than ω B97X.	S3
3.	Table S3 for the NTO1(2) of the first 10 SO-hosted singlet excitations of ideal dTpdT calculated by TD- ω B97X with large basis set 6-311+G(df,p).	S5
4.	Table S4 for the standard-orbitals projection coefficients or coefficients square of NTO1(2)-H(E) of several SO-hosted excitations of ideal Thy, dT, dTpdT, dTpdT--dApdA, and dApdTpdTpdG calculated by TD- ω B97X.	S6
5.	Figure S1 for the various molecular segments extracted from X-ray diffraction determined B-DNA (PDB code 3BSE).	S8
6.	Figure S2 for a plot of conformation comparison between ideal and 3BSE dTpdT.	S8
7.	Figure S3 for the calculated absorption spectra of various ideal/3BSE thymine-comprised systems.	S9

TABLE S1: The major internal coordinates of DNA backbone – nucleic-acid torsion angles – of ideal and 3BSE dTpdT shown in Figure 1 and S1, adopted from the conventions defined in Chap. 5 of Ref. S1. The major differences of backbone bending of the two conformations evidently come from the deviations of δ_{T1} , ϵ_{T1} and β_{T2} . However, all the torsion-angles of the two dTpdTs are fairly within the common ranges of B-DNA structures, as can be referenced in p.132 of Ref. S1.

		Ideal dTpdT	3BSE dTpdT	
Angle	Sequence	Value(°)	Value(°)	Difference(°)
β_{T1}	H*-O5'-C5'-C4'	-146.02040	-171.79766	-25.77726
γ_{T1}	O5'-C5'-C4'-	36.36158	40.98660	4.62502
δ_{T1}	C5'-C4'-C3'-	156.40092	132.93283	-23.46809
ϵ_{T1}	C4'-C3'-O3'-P	154.98268	-172.21242	32.8049
ζ_{T1}	C3'-O3'-P-O5'	-95.17465	-109.65894	-14.48429
α_{T2}	O3'-P-O5'-C5'	-46.83902	-43.83471	3.00431
β_{T2}	P-O5'-C5'-C4'	-146.00015	172.24216	-41.75769
γ_{T2}	O5'-C5'-C4'-	36.37464	36.97245	0.59781
δ_{T2}	C5'-C4'-C3'-	156.39855	146.88308	-9.51547
ϵ_{T2}	C4'-C3'-O3'-H*	154.94931	-115.74378	89.30691
χ_{T1}	O4'-C1'-N1-C2	-97.99829	-110.05868	-12.06039
χ_{T2}	O4'-C1'-N1-C2	-98.01020	-97.36020	0.65000

H* denotes that P atom is replaced with H atom.

TABLE S2: The excitation properties of ideal di-Thy, dTpdT, dTpdT--dApdA, and dApdTpdTpdG (Figure 1) provided by QNTO analysis and TDDFT with global hybrid (B3LYP^{S2, S3} and PBE1PBE^{S4}) and LC hybrid (CAM-B3LYP^{S5}, ω B97X-D^{S6}, and LC- ω PBE^{S7}) functionals other than ω B97X^{S8}. N denotes excitation order, whereas P denotes NTO2 phase for cases where NTO1 has less than 70% domination to the whole excitation. λ (nm) and f stand for absorption wavelength and oscillator strength, respectively. NTO1(2) and % record the expression of transition origin of the first (second) NTO pair and its domination to the whole excitation. Type denotes the excitation classification based on the EOM-CCSD Thy NTO1 expressions used in Ref. S9. The local Type-A, B and C derived excitations are marked in bold-face font in the N column. The data for ideal di-Thy and dTpdT is shown in (a), while that for ideal dTpdT--dApdA and dApdTpdTpdG is shown in (b).

(a)	Ideal di-Thy						Ideal dTpdT					
	N	λ (nm)	f	NTO1	%	Type	N; P	λ (nm)	f	NTO1(2)	%	Type
TD-B3LYP	1	272.81	0.0001	N1t1 - S1t1	98	A1	5	274.25	0.0189	P1t2 - S1t1	99	B21
	2	272.37	0.0009	N1t2 - S1t2	98	A2	6	267.83	0.0316	P1t1(2) - S1t2	98	(B2B12)
	3	267.89	0.0161	P1t1 - S1t2	99	B12	7	263.11	0.0005	N1t1 - S1t1	99	A1
	4	260.52	0.0232	P1t2 - S1t1	99	B21	8	262.12	0.0057	N1t2 - S1t2	99	A2
	5	249.98	0.0757	P1t2 - S1t2	96	B2	11	255.72	0.0203	P1t12 (B) - S1t1(2)	83	(B2)
	6	243.91	0.1049	P1t1(2) - S1t1	94	(B1)	12	253.85	0.2065	P1t1(2) (B) - S1t1(2)	80	(B1)
	7	238.23	0.0025	N1t1 - S1t2	99	A12	17	232.88	0.0008	N1t2 - S1t1	100	A21
	8	234.27	0.0017	N1t2 - S1t1	99	A21	19	228.83	0.0011	N1t1 (B) - S1t2	95	(A12)
	9	220.52	0	N2t2 - S1t2	95	F2	22	224.93	0.0060	N2t1 B - S1t1	93	(F1)
	10	215.67	0.0027	P2t1(2) - S1t2	98	(D2D12)	25	211.56	0.0007	(N1t1) (N2t1) B - S1t2	82	(F12)
TD-PBE1PBE	1	265.49	0	N1t1 - S1t1	10	A1	5	261.58	0.0309	P1t1(2) - S1t1	99	(B1B21)
	2	264.73	0.0002	N1t2 - S1t2	99	A2	6	257.30	0.0648	P1t1(2) (N1t2) - S1t2	95	(B2B12)
	3	255.82	0.0349	P1t1(2) - S1t2	99	(B2B12)	7	255.94	0.0004	N1t1 - S1t1	98	A1
	4	248.99	0.0395	P1t1(2) - S1t1	99	(B1B21)	8	255.33	0.0255	(P1t2) N1t2 - S1t2	97	(A2)
	5	243.88	0.0802	P1t1(2) - S1t2	97	(B2)	9	248.66	0.0354	P1t1(2) - S1t1(2)	96	(B1)
	6	237.59	0.0932	P1t1(2) - S1t1	96	(B1)	10	247.18	0.1753	P1t12 - S1t1(2)	93	(B2)
	7	223.87	0.0014	N1t1 - S1t2	99	A12	17	219.53	0.0006	N1t2 - S1t1	97	A21
	8	220.75	0.0012	N1t2 - S1t1	99	A21	18	217.66	0.0024	N1t1 B - S1t2	80	(A12)
	9	211.45	0	N2t2 - S1t2	92	F2	19	216.99	0.0097	(N1t1) (N2t2) B - S1t2	69	(A12)
	10	206.51	0.0113	P2t12 - S1t2	95	D2D12	-			N2t1 B - S1t1	27	
						20	215.09	0.0021	(N1t1) (N2t1) B - S1t2	72	(AF1AF12)	
TD-CAM-B3LYP	1	251.57	0.0001	N1t1 - S1t1	10	A1	1	244.85	0.0289	P1t1(2) - S1t1(2)	66	(B2)
	2	249.81	0.0001	N1t2 - S1t2	99	A2	-			P1t1(2) - S1t1(2)	31	
	3	238.34	0.1195	P1t2 - S1t2	95	B2	2	242.47	0.0027	N1t2 - S1t2	97	A2
	4	234.13	0.1854	P1t1 - S1t1	95	B1	3	242.10	0.0015	N1t1 - S1t1	98	A1
	5	210.53	0.0036	P1t1 - S1t2	99	B12	4	241.83	0.3783	P1t12 - S1t1(2)	64	(B1)
	6	201.23	0.0122	P1t2 - S1t1	99	B21	+			P1t1(2) - S1t1(2)	32	
	7	196.48	0.0000	N1t2 N2t2 - (S1t2) S2t2	96	C2	8	210.42	0.0052	P1t2 - S1t1	75	B21
	8	195.78	0.0010	N1t1 N2t1 - (S1t1) S2t1	96	C1	9	210.00	0.0206	P1t1 - S1t2	76	B12
	9	189.87	0.0304	P2t2 - S1t2	94	D2	11	197.09	0.0002	N1t1 N2t1 - (S1t1) S2t1	94	C1
	10	187.33	0.0664	P2t1 - S1t1	90	D1	12	193.18	0.0008	N1t2 N2t2 - (S1t2) S2t2	92	C2
						14	188.62	0.0689	P1t2 - S2t2	82	E2	
						15	186.21	0.1807	P1t1 - S2t1	69	E1	
						-			P1t2 - (S1t1) S2t2	14		
TD- ω B97X-D	1	251.79	0.0001	N1t1 - S1t1	99	A1	1	245.02	0.0308	P1t2 - S1t1(2)	67	(B2)
	2	250.28	0.0001	N1t2 - S1t2	99	A2	-			P1t1(2) - S1t1(2)	30	
	3	238.31	0.1165	P1t2 - S1t2	95	B2	2	242.79	0.0014	N1t2 - S1t2	98	A2
	4	234.29	0.1851	P1t1 - S1t1	95	B1	3	242.20	0.0024	N1t1 - S1t1	98	A1
	5	207.47	0.0044	P1t1 - S1t2	99	B12	4	242.01	0.3728	P1t1(2) - S1t1(2)	66	(B1)
	6	197.42	0.013	P1t2 - S1t1	96	B21	+			P1t1(2) - S1t1(2)	30	
	7	196.13	0	N1t2 N2t2 - S1t2 S2t2	96	(C2)	7	207.83	0.0080	P1t1 (B) - S1t2	98	(B12)
	8	195.44	0.0027	N1t1 N2t1 - (S1t1) S2t1	92	C1	9	205.77	0.0223	P1t2 - S1t1	98	B21
	9	190.73	0.0299	P2t2 - S1t2	93	D2	10	197.00	0.0002	N1t1 N2t1 - (S1t1) S2t1	94	C1
	10	188.28	0.0649	P2t1 - S1t1	90	D1	11	192.95	0.0006	N1t2 N2t2 (B) - S1t2 S2t2	91	(C2)
						13	188.64	0.0746	P1t2 - S2t2	81	E2	
						14	186.38	0.1590	P1t1 - S2t1	57	E1	
						-			P2t1 - S1t1	27		
TD-LC- ω PBE	1	243.68	0.0001	N1t1 - S1t1 (S2t1)	99	(A1)	1	236.57	0.0361	P1t2 - S1t2	66	B2
	2	241.97	0.0001	N1t2 - S1t2 (S2t2)	99	(A2)	-			P1t1 - S1t1	31	
	3	230.23	0.1279	P1t2 - S1t2	94	B2	2	235.8	0.0015	N1t2 - S1t2 (S2t2)	96	(A2)
	4	226.36	0.2347	P1t1 - S1t1	93	B1	3	234.58	0.0002	N1t1 - S1t1 (S2t1)	98	(A1)
	5	192.22	0	(N1t2) N2t2 - (S1t2) S2t2	99	(C2)	4	233.55	0.4402	P1t1 - S1t1	65	B1
	6	191.55	0.0002	N1t1 N2t1 - S2t1	99	(C1)	+			P1t2 - S1t2	31	
	7	180.46	0.0349	P1t1 - S1t2 S2t1	96	E1B12	5	192.6	0	(N1t1) N2t1 - S2t1	97	(C1)
	8	176.63	0.0256	P2t2 - S1t2	85	D2	6	188.95	0.0010	(N1t2) N2t2 - (S1t2) S2t2	93	(C2)
	9	174.44	0.0887	P2t1 - S1t1	84	D1	8	182.85	0.0322	P1t1 - S1t2 S2t1	83	(E1B12)
	10	172.45	0.1457	P1t2 - (S1t1) S2t2	86	(E2B21)	9	180.62	0.2195	P1t2 - (S1t1) S2t2	82	(E2B21)
						11	173.52	0.0856	P1t2 (P2t1) - S1t1 (S2t2)	87	(D1E2B21)	
						12	172.38	0.0376	P1t1 - S1t2 S2t1	53	(E1B12)	
						-			P1t2 P2t1 - S1t1	40		

(b)	Ideal dTpdT--dApdA						Ideal dApdTpdTpdG					
	N; P	λ (nm)	f	NTO1(2)	%	Type	N; P	λ (nm)	f	NTO1(2)	%	Type
TD-CAM- B3LYP	1	248.08	0.0246	P1t(1)2 - S1t(1)2	69	(B2)	1	249.26	0.0606	P1t1 - S1t1	86	B1
	-			P1t1(2) - S1t1(2)	28		3	244.73	0.2370	P1t2 - S1t2	53	B2
	2	245.12	0.3755	P1t1(2) - S1t1	66	(B1)	+			G - G	36	
	+			P1t(1)2 - S1t2	30		4	237.64	0.0004	N1t1 - S1t1	95	A1
	3	231.39	0.0002	N1t1 - S1t1	97	A1	5	237.33	0.0002	N1t2 - S1t2	97	A2
	4	230.04	0.0001	N1t2 - S1t2	97	A2	16	221.42	0.0069	P1t2 - S1t1	81	B21
	14	214.76	0.0292	P1t2 - S1t1	67	B21	35	203.45	0.0117	P1t1 - S1t2	90	B12
	+			A2 - S1t2	29		43	197.10	0.0005	N1t1 N2t1 (B) - S1t1 S2t1	82	(C1)
	18	206.77	0.0019	P1t1 - S1t2	69	B12	50	192.42	0.0400	P1t2 - S2t2	68	E2
	+			A1 - A2	30		+			P1t1 (B) - (S1t2) G	16	
	23	198.63	0	(N1t1) N2t1 (B) - S1t1 S2t1	86	(C1)	53	191.51	0.0107	(N1t2) (N2t2) B - (S1t2) S2t2 G	49	(C2)
	28	195.30	0.0004	(N1t2) N2t2 (B) - S1t2 S2t2	86	(C2)	+			(N2t2) B - (S2t2) G	38	
	30	191.51	0.0131	P2t1 - S1t1	82	D1	60	187.90	0.0864	P1t12 - S2t1	59	(E1E21)
32	190.77	0.0086	N2t1 (P2t1) (B) (A1) - S1t1 (S2t1)	76	(F1D1)	+			P1t1(2) B - A	28		
TD- ωB97X-D	1	248.30	0.0302	P1t2 - S1t2	71	B2	1	249.23	0.0587	P1t1 - S1t1	85	B1
	2	245.30	0.3651	P1t1 - S1t1	69	B1	2	245.46	0.1624	P1t2 - S1t2	70	B2
	+			P1t2 - S1t2	26		4	237.87	0.0002	N1t1 - S1t1	96	A1
	3	231.48	0.0001	N1t1 - S1t1	97	A1	5	237.56	0.0001	N1t2 - S1t2	96	A2
	4	230.35	0.0001	N1t2 - S1t2	97	A2	15	216.21	0.0296	P1t2 (B) - S1t1	96	B21
	13	210.21	0.0148	P1t2 - S1t1	99	B21	27	200.77	0.0099	P1t1 (B) - S1t2 (A)	93	(B12)
	17	204.45	0.0030	P1t1 - S1t2	76	B12	30	197.19	0.0002	N1t1 N2t1 (B) - S1t1 S2t1	79	(C1)
	21	198.53	0.0002	(N1t1) N2t1 A2 - S1t1 (S2t1)	68	(C1)	36	192.25	0.0023	(N1t2) N2t2 B - S1t2 S2t2	73	(C2)
	+			(N1t1) (N2t1) A2 - S2t1 A1	21		37	191.61	0.0732	P1t2 - S2t2	75	E2
	25	195.18	0.0007	(N1t2) N2t2 (B) - S1t2 (S2t2)	84	(C2)	46	186.99	0.1200	P1t1(2) - (S1t2) S2t1	71	(E1B12E 21)
	26	192.00	0.0152	P2t1 - S1t1	82	D1						
	27	191.06	0.0093	N2t1 (P2t1) (B) - S1t1 (S2t1)	81	(F1D1)						
	TD-LC- ωPBE	1	239.11	0.0366	P1t2 - S1t2	70	B2	1	240.07	0.0436	P1t1 - S1t1	75
2		236.36	0.4199	P1t1 - S1t1	69	B1	2	236.91	0.2569	P1t2 - S1t2	75	B2
+				P1t2 - S1t2	26		4	231.02	0.0001	N1t2 - S1t2 (S2t2)	96	(A2)
3		223.01	0.0001	N1t1 - S1t1 (S2t1)	95	(A1)	5	230.58	0.0002	N1t1 - S1t1 (S2t1)	95	(A1)
4		222.54	0.0001	N1t2 - S1t2 (S2t2)	96	(A2)	13	191.95	0	(N1t1) N2t1 - (S1t1) S2t1	94	(C1)
11		193.57	0	(N1t1) N2t1 - S2t1	95	(C1)	16	187.27	0.0080	(N1t2) N2t2 - S2t2	86	(C2)
13		190.56	0.0003	(N1t2) N2t2 - S2t2	95	(C2)	17	186.33	0.0405	P1t2 - S1t1 S2t2	67	E2B21
16		182.39	0.0216	(P1t2) P2t1 (A1) - S1t1	62	(D1B21)	-			A - A	11	
+				A1 (A2) - A1	12		21	183.11	0.0967	P1t1 (B) - (S1t2) S2t1 (A)	71	(E1B12)
18		181.19	0.0461	P1t1 B - S1t2 (S2t1)	71	(E1B12)	23	180.92	0.0294	P1t2 B - S1t1 (G)	77	(B21)
19		180.79	0.0006	(P1t2) (P2t2) A1 (A2) - S1t1(2) (S2t2) (A2)	41	-	24	180.36	0.0067	P1t2 B - S1t1	82	(B21)
+				P2t2 (A1) (A2) - S1t1(2) (A2)	27							
20		180.07	0.0412	P1t2 - S1t1 (S2t2)	43	(E2B21)						
+			B - S1t2	26								

TABLE S3: The NTO1(2) of the first 10 SO-hosted singlet excitations of ideal dTpdT calculated by TD- ω B97X with large basis set 6-311+G(df,p). The excitation of each system is referenced to that of the ideal system (referred to as the core molecular unit) shown in the subtitle recording the system name if an excitation correspondence is identified. For instance, the 3rd excitation (Type-A2) of dTpdT is referenced to the 2nd excitation of di-Thy, while the 9th excitation (Type-E2B21) of dTpdT, having no similar type of excitation in di-Thy, is not referenced to any excitation. The transition origin variation is denoted as σ_B (basis set resulted deviation). The local Type-A, B and C derived excitations that can be clearly recognized are marked with shadow background in the N column.

N; P	λ (nm) ; Diff. (%) of Energy	f ; Diff. (%) of f	NT01	σ_B	%	Type		
1	248.72	-4	0.0331	-11	P1t2 - S1t2	0.019	62	B2
-					P1t1 - S1t1		34	
2	245.49	-4	0.4171	0	P1t1(2) - S1t1(2)	0.044	64	(B1)
+					P1t(1)2 - S1t(1)2		32	
3	236.75	0	0.0001	-	N1t2 - S1t2 (S2t2)	0.021	95	(A2)
4	236.56	-1	0	-	N1t1 - S1t1	0.010	96	A1
6	194.33	-2	0.0169	-42	P1t1 (B) - S1t2 S2t1	0.033	81	(E1B12)
7	193.20	-1	0.0013	-	N1t1 N2t1 - (S1t1) S2t1	0.027	91	C1
8	192.30	-3	0.1237	159	P1t2 - S1t1 S2t2	0.119	85	E2B21
10	189.92	-1	0.0050	-	(N1t2) N2t2 - (S1t2) S2t2	0.057	64	(C2)
+					B - O		21	
13	184.59	-3	0.0782	-14	P1t2 - S1t1 S2t2 (O)	0.036	88	(E2B21)
15	182.63	-	0.0978	-	P1t1 - S1t2 S2t1 (O)	-	56	(E1B12)
-					P2t1 B - S1t1		36	

Basis Set Dependence of TD- ω B97X Calculation for dTpdT – 6-31G(d) vs. 6-311+G(df,p)

As shown in Table S3, the first 9 SO-hosted excitations given by 6-311+G(df,p) calculation each has a corresponding one in the 6-31G(d) result (Table 1(b)) and only the Type-E2B21 among them has a rather pronounced σ_B to be 0.119, which is also reflected in its transition expression of 6-31G(d) result bearing additional backbone-orbital involvement. As for the excitation order, we see that difference mainly arises from the CT Type-B involved excitations, i.e. switch of Type-E1B12 and Type-C1, and Type-E2B21 and Type-C2; the higher-lying Type-B21 is also replaced by a Type-E1B12. With regard to excitation energy, the local Type-As and Type-Cs (¹n π^* -character) have values almost unchanged, while the two local Type-Bs (¹ $\pi\pi^*$ -character) both have 4% lowering and the remaining CT Type-B involved excitations have 2~3% lowering. For oscillation strength it is much retained for local Type-Bs, one of which is responsible for the brightest peak (Type-B1). On the other hand, the local Type-A, C and CT Type-B excitations have larger deviation of oscillator strength (but remain dark absorptions) except the Type-E2B21 which instead has a 159% enhancement, probably due to the 6-311+G(df,p) result excluding the backbone-orbital involvement in its transition origin.

Overall, the result of local Type-A, B and C excitations given by 6-31G(d) calculation is quite similar to those given by the much more expensive 6-311G+(df,p) calculation; more deviations come from results of CT Type-B involved excitations which have larger average electron transition distance.

TABLE S4: The detailed standard-orbitals projection coefficients or coefficients square of NTO1(2)-H(E) of several SO-hosted excitations of (a) ideal di-Thy, dTpdT, dTpdT--dApdA, and dApdTpdTpdG and (b) 3BSE dT, dTpdT, dTpdT--dApdA, and dApdTpdTpdG calculated by TD- ω B97X. For orbital-fraction from backbone, the coefficients square which corresponds to electronic density contribution is shown instead. (c) The data for the coefficients square of orbitals from adenine and/or guanine in the ideal dTpdT--dApdA and dApdTpdTpdG cases.

(a)	λ (nm)	h-orbital								(B) ²	e-orbital			
		P1 _{T1}	P1 _{T2}	N1 _{T1}	N1 _{T2}	P2 _{T1}	P2 _{T2}	N2 _{T1}	N2 _{T2}		S1 _{T1}	S1 _{T2}	S2 _{T1}	S2 _{T2}
Ideal di-Thy	244.16	-0.04	0.00	0.96	0.00	0.00	0.01	-0.29	0.00		0.93	0.02	0.31	0.03
	242.42	-0.01	-0.04	0.00	0.96	0.00	-0.01	0.01	-0.27		0.03	0.93	0.06	0.31
	232.87	-0.07	0.99	-0.01	0.04	0.00	-0.05	-0.02	0.00		0.02	0.99	0.08	-0.03
	228.92	0.99	-0.10	0.04	-0.04	0.00	-0.01	0.00	0.01		0.99	-0.05	-0.07	0.04
	191.44	0.01	0.00	0.01	0.57	0.01	0.00	-0.02	0.82		0.04	-0.39	-0.02	0.89
	190.81	-0.10	-0.02	0.60	-0.01	0.00	0.00	0.78	0.01		-0.32	0.19	0.90	0.00
	188.49	0.99	0.05	0.05	0.01	-0.09	0.06	0.05	0.01		0.04	0.89	0.45	0.03
	181.05	-0.05	0.07	0.02	0.01	-0.06	0.99	0.02	0.00		0.06	0.99	0.10	0.07
	179.55	0.05	0.71	0.00	0.02	-0.69	0.11	-0.03	0.01		0.95	-0.01	0.00	0.29
	177.84	0.08	0.69	-0.01	0.03	0.71	0.07	-0.03	-0.02		0.94	0.03	-0.02	0.33
	239.30	-0.20	0.95	0.01	0.07	0.01	-0.01	-0.02	-0.02	0.04	0.21	0.96	0.09	0.02
		0.95	0.21	-0.01	0.02	-0.02	0.01	0.01	-0.01	0.04	0.96	-0.21	-0.04	0.03
	236.23	0.94	-0.24	0.00	-0.03	-0.02	-0.01	0.01	0.02	0.04	0.96	-0.23	-0.05	0.06
		0.26	0.92	-0.02	0.17	-0.04	-0.04	-0.01	-0.04	0.04	0.23	0.95	0.08	-0.03
235.97	-0.01	-0.10	0.01	0.95	0.01	0.00	0.01	-0.27	0.00	0.03	0.91	0.06	0.33	
235.06	-0.01	0.00	0.96	-0.01	0.00	0.01	-0.27	0.00	0.00	0.92	0.02	0.32	0.04	
192.01	-0.03	-0.01	0.56	-0.01	0.00	0.00	0.79	0.01	0.04	-0.36	0.14	0.89	0.01	
189.63	0.96	0.02	0.02	0.00	-0.08	0.02	0.01	-0.03	0.05	-0.01	0.82	0.56	0.07	
188.34	-0.02	0.13	0.00	0.56	-0.01	0.00	-0.01	0.78	0.04	0.05	-0.34	-0.01	0.90	
186.74	0.05	0.72	-0.01	-0.01	-0.05	0.09	0.01	-0.04	0.45	0.92	0.02	0.00	0.36	
185.94	0.10	0.59	0.00	0.01	-0.10	0.08	-0.04	-0.01	0.61	0.94	0.04	0.02	0.29	
179.79	-0.02	0.97	-0.01	0.00	-0.08	0.06	-0.01	-0.01	0.04	0.59	-0.01	-0.08	-0.78	
Ideal dTpdT (Large Basis)	248.72	-0.21	0.94	-0.01	0.03	0.00	0.01	-0.01	0.01	0.02	0.22	0.94	0.10	0.03
		0.95	0.23	0.00	-0.02	0.02	0.00	0.00	0.00	0.04	0.95	-0.23	-0.04	0.04
	245.49	0.90	-0.33	-0.01	-0.03	0.02	-0.01	0.01	0.00	0.03	0.92	-0.33	-0.05	0.07
		0.35	0.91	0.00	0.04	-0.04	-0.02	-0.01	0.00	0.04	0.33	0.91	0.10	-0.03
	236.75	-0.02	-0.03	0.01	0.96	0.01	0.00	0.01	-0.26	0.00	0.03	0.91	0.06	0.32
	236.56	-0.01	0.00	0.96	-0.02	0.02	0.00	-0.25	0.00	0.00	0.91	0.01	0.31	0.04
	194.33	0.93	0.01	-0.05	0.01	-0.07	0.02	-0.06	-0.01	0.11	-0.02	0.79	0.58	0.06
	193.20	0.05	-0.03	0.56	-0.02	-0.01	0.00	0.79	0.00	0.06	-0.38	0.16	0.86	0.00
	192.30	0.11	0.96	0.01	0.07	-0.06	0.09	0.00	0.06	0.02	0.76	0.07	0.00	0.61
	189.92	-0.01	-0.04	0.00	0.54	-0.01	-0.01	-0.01	0.78	0.08	0.06	-0.42	-0.02	0.85
		0.16	-0.03	0.00	0.07	-0.01	0.00	0.00	0.12	0.95	-0.15	0.19	0.03	0.19
	184.59	-0.01	0.96	0.00	0.01	-0.05	0.06	0.01	-0.02	0.05	0.65	-0.01	-0.07	-0.68
	182.63	0.96	-0.06	0.01	-0.02	0.03	0.02	-0.03	0.00	0.04	-0.05	0.58	-0.74	0.03
		-0.02	0.14	0.00	0.01	0.70	-0.01	0.00	0.01	0.47	0.96	0.05	-0.01	0.08
242.05	-0.15	0.95	-0.01	0.02	0.00	-0.09	-0.01	0.01	0.04	0.15	0.96	0.08	0.08	
239.09	0.95	-0.17	0.01	-0.01	-0.09	0.00	0.01	0.00	0.04	0.98	-0.13	0.01	0.04	
224.02	0.00	0.01	0.94	0.00	0.00	0.00	-0.22	0.00	0.01	0.92	0.04	0.32	0.04	
223.27	-0.02	-0.02	0.00	0.94	0.02	0.00	0.00	-0.22	0.01	0.04	0.91	0.09	0.33	
193.00	0.02	-0.02	0.52	-0.01	-0.01	0.03	0.81	0.01	0.05	-0.37	0.17	0.88	0.01	
189.76	-0.03	0.04	0.01	0.52	0.01	-0.01	0.00	0.81	0.04	0.06	-0.36	-0.01	0.90	
188.97	0.08	0.91	0.01	-0.01	-0.13	0.07	-0.01	-0.04	0.03	0.94	0.00	0.04	0.30	
186.79	0.92	0.03	0.00	0.01	-0.19	0.03	-0.01	0.00	0.09	-0.01	0.84	0.51	0.08	
181.87	0.10	0.18	-0.04	0.01	0.57	-0.01	-0.16	-0.01	0.52	0.97	0.02	0.09	0.08	
180.96	-0.05	0.08	0.02	-0.01	0.00	0.71	0.04	-0.01	0.01	0.17	0.93	0.13	0.19	
Ideal dApdTpdTpdG	242.97	0.94	-0.17	0.03	-0.03	-0.03	-0.01	0.01	0.01	0.04	0.97	0.12	0.02	0.05
	239.62	-0.12	0.96	0.00	0.04	0.00	-0.01	-0.01	0.00	0.04	-0.12	0.97	0.10	-0.03
	231.11	-0.02	-0.02	0.02	0.96	0.01	0.01	0.00	-0.27	0.01	0.04	0.90	0.07	0.33
	230.97	-0.02	0.00	0.96	-0.03	0.01	0.00	-0.26	0.01	0.01	0.91	0.03	0.33	0.04
	194.60	0.10	0.95	0.00	0.03	-0.05	0.11	-0.02	0.01	0.06	0.90	0.00	0.02	0.36
	192.01	-0.04	-0.10	0.31	0.00	0.03	0.00	0.49	0.00	0.64	0.88	0.00	-0.42	0.04
		0.00	0.07	0.48	-0.02	-0.03	0.00	0.61	-0.01	0.39	0.38	0.18	0.85	0.06
	190.91	0.12	0.04	0.43	-0.01	-0.01	0.01	0.59	-0.01	0.44	-0.75	0.14	0.60	-0.03
		0.09	-0.10	0.34	-0.01	0.05	-0.01	0.52	0.00	0.58	0.58	0.00	0.74	0.08
	188.45	0.95	-0.08	-0.01	-0.03	-0.02	0.01	-0.03	0.00	0.05	-0.03	0.47	0.75	0.06
	186.62	0.01	0.03	0.01	0.56	-0.01	-0.02	0.00	0.78	0.05	0.04	-0.35	-0.02	0.90
	182.31	-0.05	0.95	0.00	0.00	-0.02	0.01	-0.01	-0.02	0.08	-0.26	-0.01	0.03	0.80
		0.76	0.14	0.00	-0.04	-0.08	0.15	0.01	-0.03	0.32	-0.08	0.58	0.24	0.25

(b)	λ (nm)	h-orbital								(B) ²	e-orbital				
		P1 _{T1}	P1 _{T2}	N1 _{T1}	N1 _{T2}	P2 _{T1}	P2 _{T2}	N2 _{T1}	N2 _{T2}		S1 _{T1}	S1 _{T2}	S2 _{T1}	S2 _{T2}	
3BSE dT	238.04	0.00	0.04	0.00	0.95	0.00	-0.02	0.00	-0.31	0.00	0.00	0.92	0.00	0.32	
	228.90	0.00	0.98	0.00	-0.04	0.00	-0.02	0.00	0.02	0.03	0.00	0.99	0.00	-0.04	
	191.10	0.00	0.09	0.00	0.59	0.00	0.05	0.00	0.77	0.03	0.00	-0.34	0.00	0.90	
	176.81	0.00	0.07	0.00	0.02	0.00	0.98	0.00	0.03	0.01	0.00	0.99	0.00	0.11	
	176.06	0.00	0.98	0.00	-0.06	0.00	0.00	0.00	-0.05	0.03	0.00	0.02	0.00	0.99	
	168.14	0.00	0.00	0.00	0.22	0.00	-0.06	0.00	0.73	0.33	0.00	0.95	0.00	0.25	
	158.79	0.00	0.02	0.00	0.40	0.00	-0.01	0.00	-0.65	0.31	0.00	-0.85	0.00	0.48	
	157.45	0.00	-0.01	0.00	0.72	0.00	-0.03	0.00	0.04	0.44	0.00	0.86	0.00	-0.44	
		0.00	0.08	0.00	0.37	0.00	-0.10	0.00	-0.85	0.11	0.00	0.46	0.00	0.86	
	3BSE dTpdT	238.34	-0.04	0.00	0.95	0.00	0.02	0.01	-0.28	0.00	0.00	0.92	0.02	0.32	0.00
		235.85	0.84	-0.43	0.07	-0.21	-0.03	-0.02	-0.01	0.07	0.03	0.87	0.47	-0.02	0.05
			0.48	0.73	0.04	0.41	0.00	-0.03	-0.01	-0.13	0.03	-0.48	0.86	0.05	0.08
		234.90	0.00	-0.13	0.00	0.94	0.00	-0.03	0.00	-0.30	0.00	0.01	0.92	0.01	0.32
		231.25	-0.19	0.95	0.00	-0.10	0.02	-0.03	-0.01	0.02	0.03	-0.18	0.97	0.03	-0.05
		0.95	0.19	-0.03	-0.04	-0.05	-0.02	0.01	0.00	0.04	0.97	0.18	0.01	0.00	
193.05		-0.02	0.00	0.56	0.00	-0.01	0.00	0.78	-0.01	0.05	-0.36	0.03	0.90	-0.01	
190.86		0.00	0.10	0.00	0.57	0.01	0.05	0.00	0.76	0.06	0.01	-0.40	0.00	0.88	
186.03	0.95	0.05	-0.01	0.01	-0.05	-0.04	-0.01	0.01	0.07	0.01	0.96	0.23	0.04		

	181.59	0.07	0.92	-0.01	0.02	0.23	0.11	0.00	-0.01	0.08	0.94	0.01	-0.02	0.30
	178.62	0.91	-0.03	0.00	0.01	0.26	0.01	-0.06	0.02	0.06	0.26	-0.23	0.92	0.04
		-0.27	0.47	-0.05	0.00	0.78	0.05	-0.11	-0.01	0.06	-0.89	-0.08	0.22	0.37
	177.66	-0.29	-0.22	-0.01	-0.01	0.92	0.03	0.03	0.00	0.01	0.93	-0.09	0.30	0.08
		0.87	-0.20	0.02	-0.03	0.24	-0.27	0.01	-0.04	0.05	0.31	0.38	-0.85	0.13
3BSE dTpdT-- dApdA	237.57	0.95	-0.13	-0.01	-0.02	-0.11	-0.02	0.00	0.01	0.04	0.98	0.10	0.01	0.02
	233.73	-0.10	0.96	0.00	0.07	0.02	-0.08	0.00	0.00	0.03	-0.10	0.98	0.03	0.00
	229.09	-0.01	0.01	0.94	0.00	0.02	0.00	-0.25	-0.02	0.00	0.93	0.02	0.31	0.02
	226.27	-0.01	-0.06	0.00	0.94	0.00	0.00	0.01	-0.27	0.00	0.00	0.92	0.02	0.32
	193.23	-0.01	0.00	0.54	0.00	-0.02	0.00	0.80	0.01	0.05	-0.37	0.02	0.90	-0.02
	191.59	0.00	0.08	0.00	0.55	0.00	0.04	-0.01	0.78	0.05	0.00	-0.41	0.01	0.88
	188.03	0.08	0.27	0.01	0.01	0.62	0.05	-0.01	0.00	0.01	0.96	0.01	0.12	0.02
	186.87	0.06	0.01	-0.02	-0.02	0.59	-0.07	-0.04	0.01	0.03	0.89	0.21	0.13	0.05
		-0.01	0.00	0.04	0.01	-0.29	0.00	-0.02	0.02	0.03	0.34	-0.01	0.05	-0.01
	185.89	0.12	0.41	-0.01	0.02	0.47	-0.08	-0.03	0.01	0.03	0.91	-0.23	0.08	0.02
	-0.17	0.28	-0.04	0.00	0.32	0.72	0.00	0.02	0.02	0.32	0.85	0.02	0.12	
184.98	0.03	0.80	0.00	0.04	-0.28	0.04	-0.03	0.00	0.26	0.98	-0.03	0.03	0.11	
240.60	-0.11	0.95	-0.01	-0.02	-0.02	-0.02	0.00	-0.01	0.05	0.08	0.98	0.03	-0.01	
3BSE dApdTp dTpG	234.53	0.96	-0.08	0.02	0.00	-0.03	0.02	0.03	0.00	0.04	0.98	-0.06	-0.04	0.03
	232.87	0.00	0.03	0.01	0.82	0.01	-0.01	-0.01	-0.17	0.00	0.03	0.91	0.03	0.34
	226.80	-0.02	-0.02	0.79	0.01	0.01	0.01	-0.30	0.00	0.01	0.90	0.01	0.32	0.02
	194.66	-0.01	0.10	0.00	0.41	0.00	-0.01	0.00	0.69	0.10	0.00	-0.47	0.00	0.84
	190.65	0.10	-0.02	0.48	-0.01	0.04	0.00	0.57	0.00	0.16	-0.51	0.03	0.81	-0.03
	188.88	0.96	0.08	0.02	-0.01	0.09	0.09	0.02	-0.01	0.03	0.00	0.96	0.17	0.01
	183.95	0.93	-0.06	-0.05	0.00	-0.04	0.02	-0.03	-0.01	0.08	0.03	-0.18	0.56	0.02
	182.17	0.07	0.88	0.00	-0.01	-0.03	-0.03	0.02	-0.01	0.19	0.90	-0.03	0.05	0.27
		-0.12	0.26	0.00	0.00	0.00	0.01	0.00	0.00	0.91	0.22	-0.01	-0.02	0.09
	176.83	-0.08	0.02	0.01	0.01	0.01	0.88	-0.02	0.05	0.18	0.13	0.97	0.03	0.07
	0.07	-0.01	0.02	0.00	-0.18	-0.18	0.03	-0.01	0.92	0.97	-0.13	-0.02	0.00	

(c)	dTpdT--dApdA					dApdTpTpG				
	λ (nm)	h-orbital		e-orbital		λ (nm)	h-orbital		e-orbital	
		(A1)	(A2)	(A1)	(A2)		(G) ²	(A) ²	(G) ²	(A) ²
Ideal	242.05	0.00	0.00	0.00	0.00	242.97	0.00	0.01	0.00	0.01
	239.09	0.00	0.00	0.00	0.00	239.62	0.00	0.00	0.00	0.00
	224.02	0.05	0.00	0.00	0.00	231.11	0.00	0.00	0.00	0.00
	223.27	0.00	0.05	0.00	0.00	230.97	0.00	0.00	0.00	0.01
	193.00	0.00	0.00	0.00	0.00	194.60	0.00	0.00	0.03	0.01
	189.76	0.00	0.00	0.00	0.00	192.01	0.00	0.00	0.00	0.02
	188.97	0.08	0.01	0.00	0.00		0.00	0.00	0.00	0.02
	186.79	0.00	0.00	0.00	0.00	190.91	0.00	0.00	0.00	0.02
	181.87	0.05	0.02	0.00	0.00		0.00	0.00	0.00	0.04
	180.96	0.01	0.45	0.02	0.01	188.45	0.00	0.01	0.00	0.19
						186.62	0.00	0.00	0.01	0.00
						182.31	0.00	0.00	0.26	0.00
							0.01	0.03	0.25	0.25
	3BSE	237.57	0.00	0.00	0.00	0.00	240.60	0.00	0.01	0.00
233.73		0.00	0.00	0.00	0.00	234.53	0.00	0.00	0.00	0.00
229.09		0.03	0.00	0.01	0.00	232.87	0.00	0.00	0.00	0.00
226.27		0.00	0.04	0.00	0.01	226.80	0.00	0.00	0.00	0.00
193.23		0.01	0.00	0.00	0.00	194.66	0.00	0.00	0.00	0.02
191.59		0.00	0.01	0.00	0.00	190.65	0.00	0.00	0.01	0.00
188.03		0.39	0.11	0.02	0.01	188.88	0.00	0.00	0.00	0.01
186.87		0.18	0.43	0.12	0.00	183.95	0.00	0.00	0.63	0.00
		0.84	0.02	0.84	0.01	182.17	0.00	0.01	0.06	0.01
185.89		0.18	0.37	0.06	0.02		0.00	0.00	0.91	0.00
		0.04	0.19	0.12	0.02	176.83	0.00	0.02	0.00	0.01
184.98		0.00	0.01	0.00	0.00		0.00	0.00	0.00	0.00

Figure S1. Various molecular segments extracted from X-ray diffraction determined B-DNA (PDB code 3BSE). The structures of (a) dT, (b) dTpdT, (c) dTpdT--dApdA, and (d) dApdTpdTpdG under study are shown.

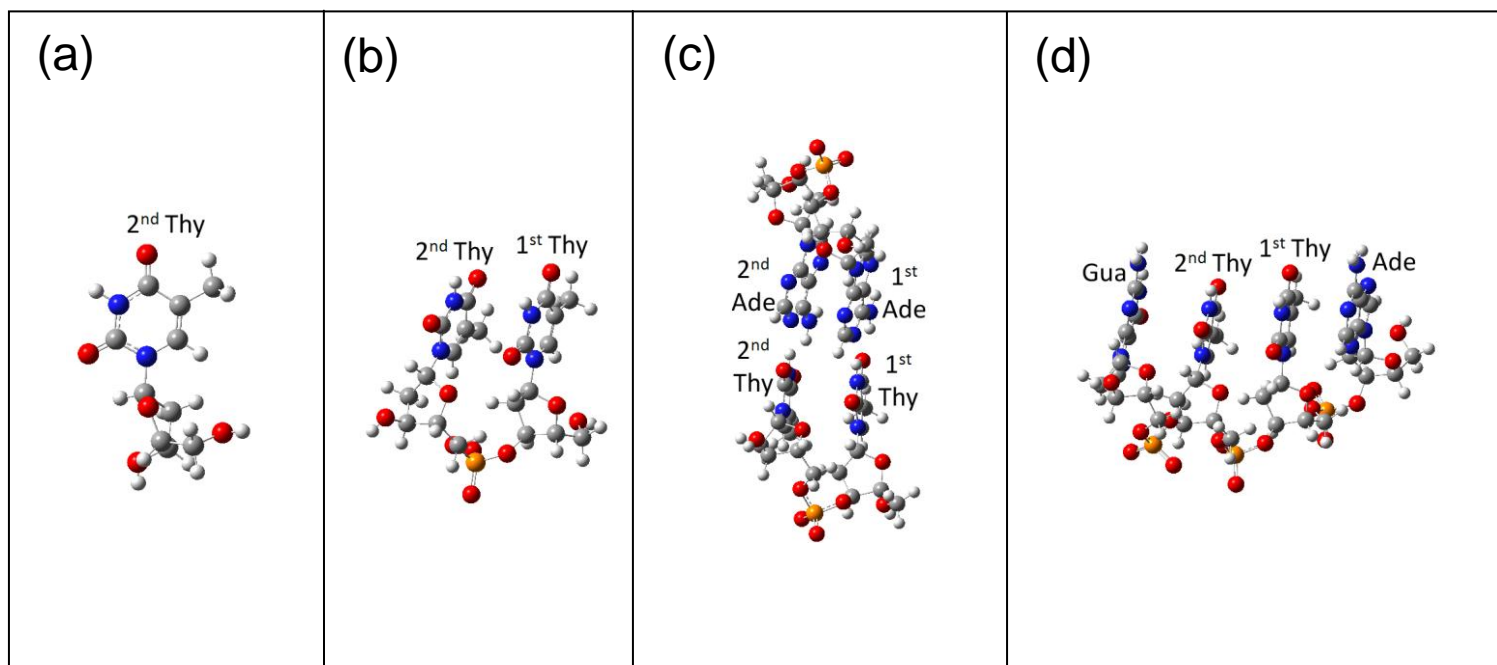
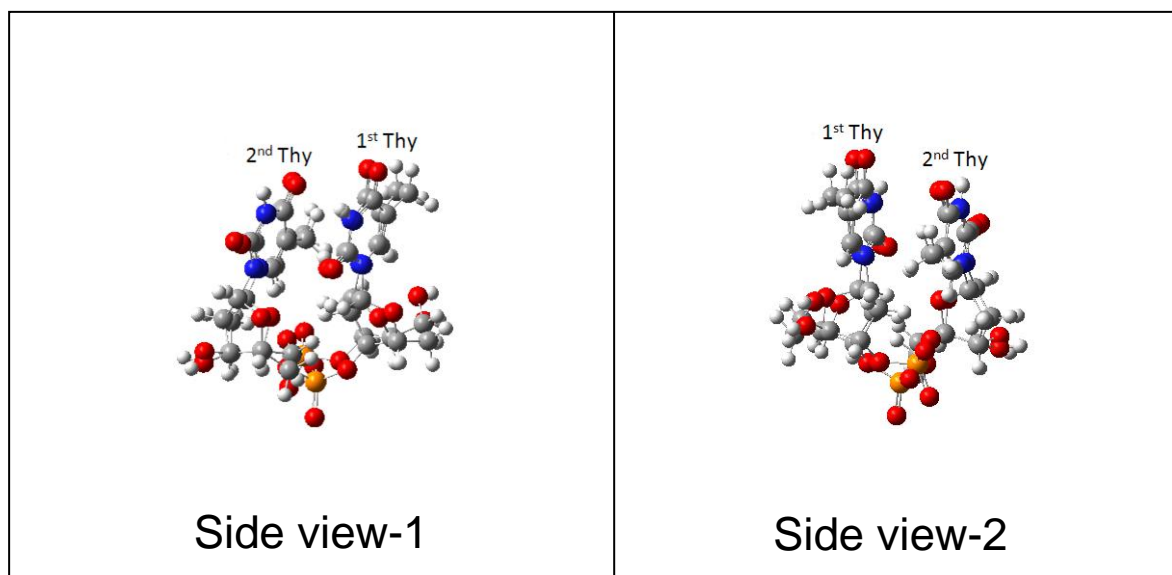


Figure S2. Comparison of conformation between ideal and 3BSE dTpdT where the two molecules are superimposed together. The major difference can be found in the backbone bending which in turn results in a small deviation of the base-plane angle. Nonetheless, the important coordinate, *i.e.*, distance between the two thymines, has not deviated strongly from each other. The difference of ground state energy calculated (6-31G(d) DFT/B3LYP) is 0.205eV (3BSE one has lower energy).



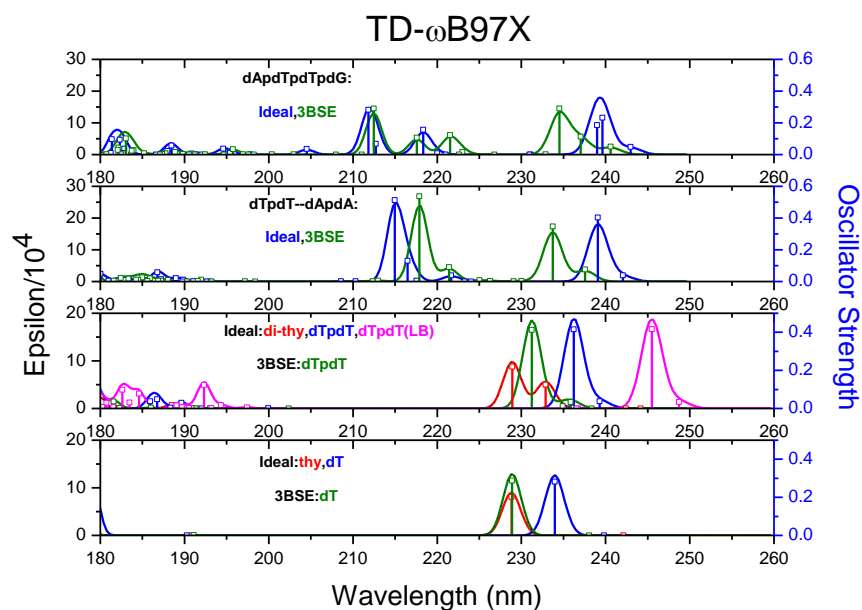


Figure S3 The calculated absorption spectra of various thymine-comprised ideal/3BSE systems. Each resonance peak is broadened with a Lorentzian with a 0.03eV of Half-Width at Half Height.

References

- (S1) T. Schlick, *Molecular Modeling and Simulation*; Springer, New York, 2002.
 (S2) A. D. Becke, *J. Chem. Phys.*, 1993, **98**, 5648.
 (S3) C. Lee, W. Yang and R. G. Parr, *Phys. Rev. B*, 1988, **37**, 785.
 (S4) C. Adamo and V. Barone, *J. Chem. Phys.*, 1999, **110**, 6158.
 (S5) T. Yanai, D. Tew and N. Handy, *Chem. Phys. Lett.*, 2004, **393**, 51.
 (S6) J.-D. Chai and M. Head-Gordon, *Phys. Chem. Chem. Phys.*, 2008, **10**, 6615.
 (S7) O. A. Vydrov, J. Heyd, A. V. Krukau and G. E. Scuseria, *J. Chem. Phys.*, 2006, **125**, 074106.
 (S8) J.-D. Chai and M. Head-Gordon, *J. Chem. Phys.*, 2008, **128**, 084106.
 (S9) J.-H. Li, J.-D. Chai, G. Y. Guo and M. Hayashi, *Chem. Phys. Lett.*, 2011, **514**, 362.